Revisiting the Kepler problem with linear drag using the blowup method and normal form theory

Kristiansen, Kristian Uldall

Published in:
Nonlinearity

Link to article, DOI:
10.1088/1361-6544/ad2379

Publication date:
2024

Document Version
Publisher's PDF, also known as Version of record

PAPER • OPEN ACCESS

Revisiting the Kepler problem with linear drag using the blowup method and normal form theory

To cite this article: K Uldall Kristiansen 2024 *Nonlinearity* **37** 035014

OPEN ACCESS
IOP Publishing | London Mathematical Society Nonlinearity
Nonlinearity **37** (2024) 035014 (45pp) https://doi.org/10.1088/1361-6544/ad2379

Revisiting the Kepler problem with linear drag using the blowup method and normal form theory

K Uldall Kristiansen

Department of Applied Mathematics and Computer Science, Technical University of Denmark, 2800 Kgs. Lyngby, Denmark

E-mail: krkri@dtu.dk

Received 14 March 2023; revised 13 December 2023
Accepted for publication 29 January 2024
Published 9 February 2024

Recommended by Dr Tere M Seara

Abstract

In this paper, we revisit the Kepler problem with linear drag. With dissipation, the energy and the angular momentum are both decreasing, but in Margheri *et al* (2017 *Celest. Mech. Dyn. Astron.* **127** 35–48) it was shown that the eccentricity vector has a well-defined limit in the case of linear drag. This limiting eccentricity vector defines a conserved quantity, and in the present paper, we prove that the corresponding invariant sets are smooth manifolds. These results rely on normal form theory and a blowup transformation, which reveals that the invariant manifolds are (nonhyperbolic) stable sets of (limiting) periodic orbits. Moreover, we identify a separate invariant manifold which corresponds to a zero limiting eccentricity vector. This manifold is obtained as a generalized center manifold over the zero eigenspace of a zero-Hopf point. Finally, we present a detailed blowup analysis, which provides a geometric picture of the dynamics. We believe that our approach and results will have general interest in problems with blowup dynamics, including the Kepler problem with generalized nonlinear drag.

Keywords: invariant manifolds, nonhyperbolic sets, dynamical systems theory, blowup

Mathematics Subject Classification numbers: 37G05, 37N05, 37D10, 34C29

1. Introduction

In this paper, we consider the Kepler problem with linear drag [35, 36]

$$\ddot{u} + \delta\dot{u} + c\frac{u}{|u|^3} = 0, \tag{1.1}$$

with $u(t) \in \mathbb{R}^3\backslash\{0\}$, $c > 0$ and for $\delta > 0$. The singularity at $u = 0$ corresponds to the collision limit and for $\delta = 0$ (no drag/damping), we obtain the classical Kepler problem, whose orbits are conic sections. In fact, as in the classical case, we may scale u and t to achieve $c = 1$ so we will assume this henceforth. (In this way, δ is replaced by $\delta c^{-1/2}$). For $\delta = 0$, the energy:

$$E(u,\dot{u}) = K(\dot{u}) + P(u), \quad K(\dot{u}) := \frac{1}{2}|\dot{u}|^2, P(u) := -\frac{1}{|u|},$$

the angular momentum:

$$L(u,\dot{u}) = u \wedge \dot{u},$$

and the eccentricity vector

$$\mathcal{E}(u,\dot{u}) = \dot{u} \wedge L(u,\dot{u}) - \frac{u}{|u|}, \tag{1.2}$$

are all conserved quantities. For $\delta \neq 0$, we have $\frac{d}{dt}E = -\delta|\dot{u}|^2 \leqslant 0$ and hence the energy is monotonically decreasing for $\delta > 0$. Moreover, a simple calculation shows that

$$\frac{d}{dt}L = -\delta L, \tag{1.3}$$

so that

$$L(u(t),\dot{u}(t)) = e^{-\delta t}L(u(0),\dot{u}(0)), \tag{1.4}$$

and the angular momentum is therefore exponentially decreasing. Notice, however, that the direction of L is constant and the motion $(u,\dot{u})$ is therefore contained in a plane (the orbital plane).

The eccentricity $\mathcal{E}$ is also not conserved for $\delta \neq 0$, but in [36] it was shown that there exists a limiting eccentricity vector: Let $\phi_t(u,\dot{u})$ denote flow associated with (1.1). Then

$$\mathcal{E}_\infty(u,\dot{u}) = \lim_{t\to t_{\max}^-} \mathcal{E}(\phi_t(u,\dot{u})),$$

exists for all $u,\dot{u}$. Here $t_{\max}$ is the maximum time of existence (finite for $L = 0$, infinite for $L \neq 0$, see [35]). In [36], it was shown that the components of $\mathcal{E}_\infty$ are functionally independent and rotationally equivariant:

$$\mathcal{E}_\infty(Ru,R\dot{u}) = R\mathcal{E}_\infty(u,\dot{u}) \quad \forall R \in SO(3),$$

and that $|\mathcal{E}_\infty(u,\dot{u})|$ attains all values in $(0,1]$. If $|\mathcal{E}_\infty(u,\dot{u})| = 1$ then $L = 0$, see [36]. In [37], the same authors generalized their results to the case, where δ is a function $\delta(|u|)$ of $|u|$ satisfying $\delta(|u|) \geqslant c > 0$. In [33], the drag $\delta(|u|)$ was singular at $u = 0$, and they showed that in some cases, the limiting eccentricity vector can be discontinuous.

The question of smoothness of $\mathcal{E}_\infty$ for (1.1) was left open in [36]. In this paper, we will give a different characterization of $\mathcal{E}_\infty$, which will allow us to address the issue of smoothness of $|\mathcal{E}_\infty| \in (0,1)$. At the same time, using dynamical systems theory, we identify a new smooth invariant manifold corresponding to $\mathcal{E}_\infty = 0$, which acts as a center of the oscillating orbits with $|\mathcal{E}_\infty| \in (0,1)$. It should be said that this invariant manifold, which will be one-dimensional in a reduced phase space, corresponding to $\mathcal{E}_\infty = 0$, was actually derived as a formal series in [19], which sparked the interest of the present author. Essentially, our proof shows that this series is summable in the sense of Borel–Laplace. Separately, using blowup and compactification as our main tools, we provide a geometric description of the dynamics. This will shed further light on $|\mathcal{E}_\infty| \to 1$.

The study of dissipation in celestial mechanics has a long history. It even dates back to Jacobi [20], who introduced dissipative forces of the type $-\delta|\dot{u}|^{n-1}\dot{u}$; the case $n = 1$ corresponds to the linear drag studied in the present paper. There are at least two important mechanisms for dissipation in celestial mechanics: particle collisions due to nebula (Stokes' dissipation) and solar radiation (Poynting–Robertson dissipation), see [6, 35].

Corne and Rouche [8] and Diacu [9] were perhaps the first contributors towards the development of a qualitative theory of the Kepler problem with drag (1.1) for general families of non-constant drag forces $\delta = \delta(u, \dot{u})$, depending on u and $\dot{u}$. [8] considered (1.1) with $\delta(u, \dot{u}) = k(|\dot{u}|)/|\dot{u}|$ and showed, under some additional assumptions on the function k, that all solutions go to the singularity (potentially in finite time). On the other hand, [9] analyzed the qualitative dynamics of the dissipative Kepler problem within a generalized class of Stokes drag; this family includes the important Poynting–Robertson case. Many years later, Margheri, Ortega, and Rebelo in [35] studied the Kepler problem with linear drag (1.1) and provided a more thorough description of the dynamics. In particular, they proved that the system is complete, i.e. solutions exist globally in time, on the set of nonzero angular momentum. Later in [36], the same authors then provided a more geometric description, including the properties of the limiting eccentricity vector. Their results also showed that $\limsup_{t\to\infty}$ and $\liminf_{t\to\infty}$ of $|u(t)||L(t)|^{-2}$ both exist along orbits with $|\mathcal{E}_\infty| \in (0,1)$, see also [19].

In parallel, there has been some studies of dissipative versions of the restricted three body problem, see e.g. [6, 18, 34]. In [6] the authors used numerical methods (based upon Fast Lyapunov Indicators) to provide information on the different regions of the phase space. They demonstrated both collision and non-collision trajectories. Interestingly, they also documented periodic orbit attractors, but only in the case of linear and Stokes drags. In contrast, in the case of the Poynting-Robertson dissipation, the authors found no other attractors beside the primaries (collisions). Following on from this research, [34] studied the existence (and nonexistence) of periodic orbits, including Hopf bifurcations around the libration points L_4 and L_5.

In this paper, we will use the blowup method and normal form theory to study the dynamics of (1.1). In the context of celestial mechanics and Hamiltonian systems, normal form theory has a long history, dating back to the work of Poincaré and Birkhoff. In fact, KAM theory [1] itself may be viewed as a normal form theory. On the other hand, the blowup method provides a general framework for studying degenerate equilibria in local dynamical systems theory, where the hyperbolic theory (e.g. Hartman-Grobman and center manifolds) does not apply. The rough idea of this approach is to apply a non-invertible transformation (like polar coordinates) that blows up the equilibrium to a sphere (or cylinders in case of lines of degenerate equilibria). By appropriately choosing weights associated to the transformation, it is possible (at least for analytic systems) to divide the resulting vector-field by a power of the radius, measuring the distance to the equilibrium. This gives rise to a new vector-field, only equivalent to the original one away from the equilibrium, for which hyperbolicity (or ellipticity) may be

(partially) gained on the blowup of the singularity. Sometimes this approach of blowing up equilibria has to be used successively, see e.g. [14].

In recent years, this blowup approach has gained prominence within the area of singular perturbation theory, because here degenerate equilibria occur naturally, see [12, 13, 15, 31]. In combination, Fenichel's geometric singular perturbation theory and the blowup method has been very successful in describing global phenomena in slow-fast models, see e.g. [23–26, 29]. More recently, the blowup approach has been generalized with the purpose of 'gaining smoothness', rather than hyperbolicity, in the context of smooth systems approaching nonsmooth ones, see [21, 22, 27, 32].

Obviously, blowup can also take on a different meaning in mathematics, namely (finite time) blowup of solutions of (ordinary or partial) differential equations. In dynamical systems theory, blowup solutions can be studied by Poincaré or Poincaré-Lyapunov compactification (which in fact bear some resemblance to the blowup method), see [14]. Upon compactification one can study equilibria, again after proper desingularization of the vector-field, at infinity and these can be analyzed by local methods of dynamical systems theory. In particular, such points at infinity are sometimes completely degenerate, which can then be resolved by the blowup method.

Related to blowup of solutions is the existence of solutions approaching true singularities of ordinary differential equations; like the collision limit $u = 0$ for (1.1) where the associated vector-field is ill-defined. The analysis of collision (as well as near-collision) solutions in the n-body problem has a long history, also dating back to Poincaré, see also [5, 10, 11]. For the two-body problem, which can be reduced to $(1.1)_{\delta=0}$, there is a change of coordinates (the Levi–Civita transformation) and a nonlinear transformation of time (related to desingularization), that transforms the collision into a regular point of the equations. The Levi–Civita transformation is—similar to a blowup transformation—not invertible; it is in fact a double cover. More generally in the n-body problem, the Levi–Civita transformation can be applied to show that solutions of the n-body problem can be analytically continued through isolated binary collisions (this is also known as regularization in the context of celestial mechanics). Interestingly, Mcgehee [39] used the blowup method to study the more complicated triple collision in the context of the collinear three-body problem. Indeed, the author blew up the collision set to a sphere and upon applying desingularization, he obtained hyperbolic equilibria points on a collision manifold. This led the author (through hyperbolic invariant manifolds) to conclude that the triple collision cannot be regularized. Subsequently, this approach was used in [16] to show that the simultaneous binary collision scenario was C^0-regularizable. Interestingly, [38] proved that it is exactly $C^{8/3}$-regularizable in the collinear case. A separate geometric proof—based upon normal form theory and the blowup approach of [16, 39]—was given in [10]. This approach led the same authors in [11] to prove that the same results hold in the planar case, a result that was initially conjectured by [38].

While our findings on a classical problem are interesting on their own, a main goal of this work is also to create a template—leveraging blowup and normal form theory—for studying similar problems, including (1.1) for more general non-constant $\delta = \delta(u, \dot{u})$. We refer to the preprint [28] for a demonstration of the use of this template. Here the issue of circularization is solved in a broad class of damped Kepler problems.

1.1. Outline

The paper is organized as follows: In section 2, we lay out our approach (based upon certain blowup transformations) for characterizing $\mathcal{E}_\infty$ and present two theorems on the existence of smooth invariant manifolds of (1.1): theorem 2.6 for the existence of the orbit corresponding

to $\mathcal{E}_\infty = 0$ and theorem 2.7 for the existence of a smooth invariant manifold corresponding to $|\mathcal{E}_\infty| \in (0,1)$, see also theorem 2.8. We prove theorem 2.6 in section 3 using general results on Gevrey-1 invariant manifolds $y = Y(x)$ for analytic systems of the form $x^2\frac{dy}{dx} = F(x,y)$, with $F(0,0) = 0$ and $D_yF(0,0)$ non-singular. It is the author's impression that these results are not so well-known. We follow [4], which proves the existence of such manifolds (and certain normal forms) in perhaps the most accessible way. Theorem 2.7 is proven in section 4 using normal form theory (based upon averaging) to set up an appropriately regular equation for the invariant manifolds that can be solved upon application of the implicit function theorem. This approach, which is reminiscent to a flow-box argument, may have general interest. In section 5, we apply a sequence of blowup transformations along with an appropriate compactification in order to provide a geometric description of the dynamics. We summarize this in figure 1. From [36], it is known that $|\mathcal{E}_\infty|$ cannot exceed 1. The results of our blowup analysis, will provide a different characterization of this fact that also allow us to address the subtleties of $|\mathcal{E}_\infty| \to 1$. We lay this out in further details in our final discussion section, 6.

2. Existence of invariant manifolds

Since the direction of L is preserved, it is without loss of generality to consider $u(t) \in \mathbb{R}^2$. We will do so henceforth. Upon identifying $\mathbb{R}^2$ with $\mathbb{C}$ in the usual way, we put

$$u := re^{i\theta}, \tag{2.1}$$

and let

$$l := |L| = r^2\dot{\theta} \geqslant 0, \tag{2.2}$$

denote the magnitude of the angular momentum. Then (1.1) becomes

$$\begin{aligned} \ddot{r} &= -\frac{1}{r^2} + \frac{l^2}{r^3} - \delta\dot{r}, \\ \dot{l} &= -\delta l. \end{aligned} \tag{2.3}$$

Suppose first that $l > 0$, and define the coordinates r_1 and v by

$$r = l^2 r_1, \quad v = l\dot{r}. \tag{2.4}$$

These coordinates appear in a systematic way through our blowup approach, see section 5. Then the kinetic energy, K, takes the following form:

$$K(\dot{u}) = \frac{1}{2}\left(\dot{r}^2 + \frac{l^2}{r^2}\right) = \frac{1}{2l^2}\left(v^2 + \frac{1}{r_1^2}\right),$$

in the (r_1, v, l)-coordinates. Moreover, we have the following differential equations

$$\begin{aligned} \dot{r}_1 &= l^{-3}\left(v + 2\delta r_1 l^3\right), \\ \dot{v} &= l^{-3}\left(-\frac{r_1 - 1}{r_1^3} - 2\delta v l^3\right), \\ \dot{l} &= -\delta l. \end{aligned} \tag{2.5}$$

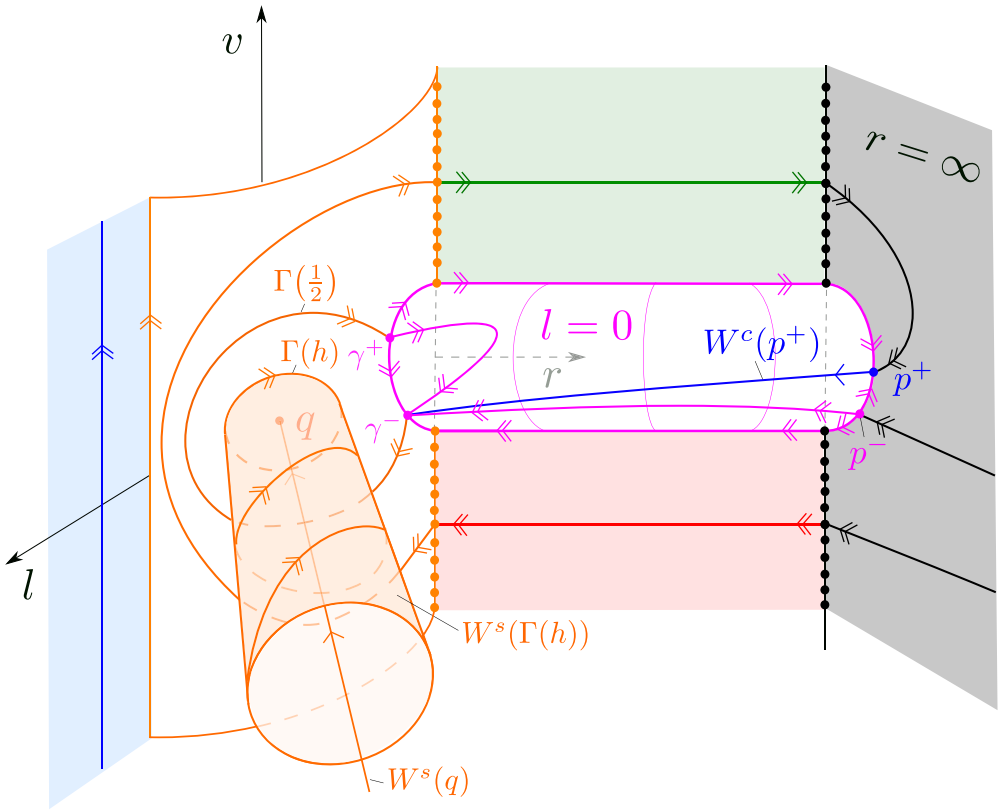

Figure 1. A geometric picture of the dynamics of (1.1) upon blowup (and desingularization). Here $l=|L|$ and v is defined by $v=l\dot{r}$, see (2.4). The invariant manifolds $W^s(q)$ and $W^s(\Gamma(h))$ are stable sets of a zero-Hopf point q and periodic orbits $\Gamma(h)$, $h\in(0,\frac{1}{2})$, respectively, on the blowup of $r=l=0$; the direction normal to $\Gamma(h)$, where $l>0$, is nonhyperbolic. $W^s(\Gamma(h))$ corresponds to $|\mathcal{E}_\infty|\in(0,1)$ whereas $W^s(q)$ corresponds to $\mathcal{E}_\infty=0$. Finally, $|\mathcal{E}_\infty|=1$ on the $l=0$-cylinder in purple. See section 5 for further details. The heteroclinic cycle $\Gamma(\frac{1}{2})$ is important for the description of $|\mathcal{E}_\infty|\to 1$, see section 6. Moreover, the heteroclinic orbits within $l=0$ connecting γ^+ and γ^- correspond to ejection-collision orbits with $r(t)\to 0$ in backwards and forward time, see [35]. On the other hand, the connections between p^- at infinity and γ^- are capture-collision orbits with $r(t)\to 0$ in backwards and forward time, see e.g. [9, 35]. The unique capture-collision connection between the nonhyperbolic saddle p^+ and γ^- is the boundary between ejection-collision and capture-collision orbits, see remark 5.7.

Now, since l^{-3} is a common factor of the right hand side, we make a nonlinear transformation of time that corresponds to multiplication by l^3:

$$\begin{aligned} r_1' &= v+2\delta r_1 l^3,\\ v' &= -\frac{r_1-1}{r_1^3}-2\delta v l^3,\\ l' &= -\delta l^4. \end{aligned} \tag{2.6}$$

(2.5) and (2.6) are equivalent for $l>0$. However, (2.6) is defined for $l=0$ (it defines an invariant set) and we can therefore use dynamical systems theory to infer properties from $l=0$ to $l>0$ by working on (2.6). In turn, this then carries over to the equivalent system (2.5).

Remark 2.1. In the following we will reserve $\dot{()}$ to denote differentiation with respect to the original time. In comparison, we will use $()'$ repeatedly to refer to differentiation with respect to different times. It should be clear form the context how different $()'$ may be related.

Setting $l=0$ in (2.6) gives

$$\begin{aligned} r_1' &= v,\\ v' &= -\frac{r_1-1}{r_1^3}, \end{aligned} \tag{2.7}$$

which is Hamiltonian with Hamiltonian function:

$$H(r_1,v)=\frac{1}{2}v^2+\frac{(r_1-1)^2}{2r_1^2}. \tag{2.8}$$

Remark 2.2. If $\delta=0$, then (1.1) reduces to the conservative Kepler problem and the Hamiltonian function (2.8), written in terms of the original variables $r,\dot{r}$ and l:

$$H\left(l^{-2}r,l\dot{r}\right)=\frac{1}{2}l^2\dot{r}^2+\frac{\left(l^2-r\right)^2}{2r^2},$$

is, along with l, a conserved quantity of (2.3). In fact, $H=\frac{1}{2}|\mathcal{E}|^2$ in this case.

Lemma 2.3. *Consider (2.1), (2.2) and (2.4). Then*

$$\dot{u}=\frac{v}{l}e^{i\theta}+\frac{il}{r}e^{i\theta},$$

and

$$e^{-i\theta}\mathcal{E}(u,\dot{u})=\frac{1-r_1}{r_1}-iv,$$

so that

$$H(r_1,v)=\frac{1}{2}|\mathcal{E}(u,\dot{u})|^2. \tag{2.9}$$

Proof. Direct calculation, recall (1.2). □

As a corollary, we have that

$$H_\infty(r_1,v,l):=\lim_{t\to\infty}H(\underline{r}_1(t,r_1,v,l),\underline{v}(t,r_1,v,l))=\frac{1}{2}|\mathcal{E}_\infty(u,\dot{u})|^2, \tag{2.10}$$

where we use $(\underline{r}_1(t,r_1,v,l),\underline{v}(t,r_1,v,l),\underline{l}(t,r_1,v,l))$ with

$$\underline{z}(0,\ldots)=z,$$

$z=r_1,v$, and l, as our notation for the flow of (2.6).

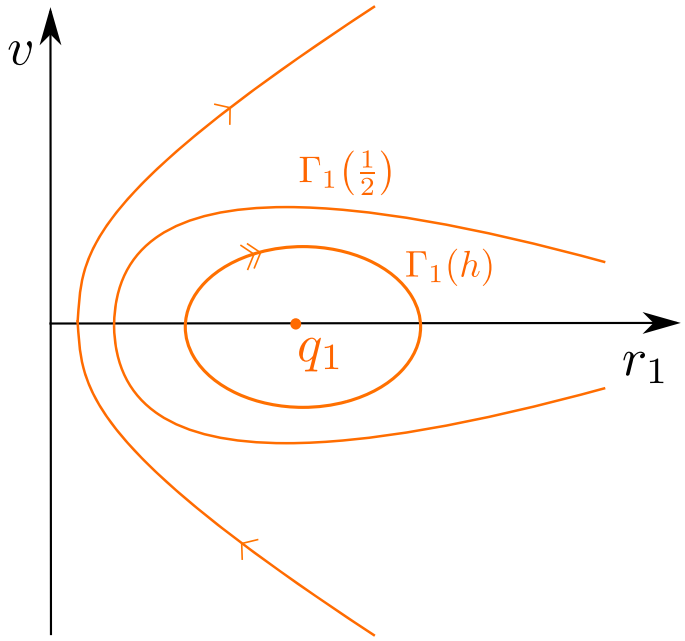

Figure 2. Phase portrait of (2.7). The orbit $\Gamma_1\left(\frac{1}{2}\right)$ defined by $H(r_1,v)=\frac{1}{2}$ is a separatrix, separating bounded from unbounded orbits.

Lemma 2.4. *$(r_1,v)=(1,0)$ is a center for (2.7), surrounded by periodic orbits $\Gamma_1(h)$, $h\in\left(0,\frac{1}{2}\right)$, given by the level sets $H(r_1,v)=h$. Here $\Gamma_1(h)$ intersects the r_1-axis in two points $(r_{1,\pm}(h),0)$ with*

$$r_{1,-}(h)=\frac{1}{1+\sqrt{2h}},\quad r_{1,+}(h)=\frac{1}{1-\sqrt{2h}}.$$

The unbounded orbit $\Gamma_1\left(\frac{1}{2}\right)$ given by the level set $H(r_1,v)=\frac{1}{2}$ (corresponding to $|\mathcal{E}|=1$ by (2.10)), intersects the r_1-axis once in $r_1=r_{1,-}(\frac{1}{2})=\frac{1}{2}$, and is a separatrix, separating the bounded orbits ($H(r_1,v)<\frac{1}{2}\Leftrightarrow|\mathcal{E}|<1$) from unbounded orbits ($H(r_1,v)>\frac{1}{2}\Leftrightarrow|\mathcal{E}|>1$).

Proof. Direct calculation. Notice in particular that $(r_1,v)=(1,0)$ is an extremum (minimum) of the Hamiltonian function and therefore also a center of (2.7). In fact, the linearization around $(r_1,v)=(1,0)$ produces $\pm i$ as the eigenvalues. □

We illustrate the phase portrait of (2.7) in figure 2.

Linearization of (2.6) at the corresponding equilibrium point q_1 of the full system, given by

$$q_1:\quad (r_1,v,l)=(1,0,0),$$

clearly produces eigenvalues $\pm i,0$. It therefore corresponds to a zero-Hopf point [17]. Similarly, all periodic orbits $\Gamma_1(h)$, $h\in\left(0,\frac{1}{2}\right)$ are also degenerate when embedded within the full system (2.6). The description of the stable sets of these sets of points is therefore complicated by the lack of hyperbolicity.

Remark 2.5. For $\delta = 0$, l and H (see remark 2.2) are both conserved quantities. In this case, q_1 corresponds to circular orbits of the (conservative) Kepler problem with zero eccentricity, whereas $\Gamma_1(h)$, $h \in (0, \frac{1}{2})$, correspond to elliptic ones with $|\mathcal{E}| \in (0,1)$. Finally, $\Gamma_1\left(\frac{1}{2}\right)$ corresponds to the parabolic orbits whereas $\Gamma_1(h)$, $h > \frac{1}{2}$ corresponds to hyperbolic ones.

2.1. Main results

We now state our main results.

Theorem 2.6 (The local stable manifold $W^s_{loc}(q_1)$ of q_1). *The local stable set $W^s_{loc}(q_1)$ is a smooth one-dimensional manifold, taking the following graph form*

$$r_1 = 1 + l^3 F_1\left(l^3\right), \quad v = l^3 G_1\left(l^3\right), \quad l \in [0, l_0], \tag{2.11}$$

for $l_0 > 0$ small enough and where $F_1, G_1 : [0, l_0] \to \mathbb{R}$ are Gevrey-1 smooth functions. Moreover,

$$\frac{d^{2n}}{dx^{2n}} F_1(0) = 0, \quad \frac{d^{2n+1}}{dx^{2n+1}} G_1(0) = 0, \tag{2.12}$$

for all $n \in \mathbb{N}_0$.

Upon using (2.4), we find that $W^s(q_1)$ in (2.11) takes the following form

$$r = l^2\left(1 + l^3 F_1\left(l^3\right)\right), \quad \dot{r} = l^2 G_1\left(l^3\right),$$

with respect to r and $\dot{r}$. These quantities are smooth functions of l along this orbit and decay like $e^{-2\delta t}$. Since $F_1(0) = 0$, see (2.12) with $n = 0$, we obtain from (1.3), (2.2) and (2.4) that

$$\frac{d\theta}{dl} = -\frac{1}{\delta l^4 (1 + l^3 F_1(l^3)} := -\frac{1}{\delta l^4}\left(1 + l^6 \widetilde{F}_1(l^3)\right), \tag{2.13}$$

and consequently that the sum

$$l^3\theta(l) + l^3 \int \frac{1}{\delta l^4} dl = l^3\theta(l) - \frac{1}{3\delta},$$

being equal to

$$-\frac{l^3}{3\delta} \int \widetilde{F}_1\left(l^3\right) dl^3,$$

by (2.13), is a smooth function of l^3 along the orbit in (2.11). This result complements results of [36, equation (43)] which showed that $\limsup_{t\to\infty}$ and $\liminf_{t\to\infty}$ of $\dot{\theta} l^{-3}$ both exist whenever $|\mathcal{E}_\infty| \in (0,1)$. Finally, we emphasize that, since the flow is regular away from $l = 0$, we can globalize the local manifold to a global one $W^s(q_1)$. In fact, since $l' < 0$ for $l > 0$ and since the system is real analytic, this global manifold is also a Gevrey-1 smooth graph over l^3. Clearly, the local stable manifold coincides with the $W^s(q_1) \cap N$ where N is a neighboorhood of q_1. This also applies the stable sets $W^s(\Gamma_1(h))$ of $\Gamma_1(h)$ with $h \in (0, \frac{1}{2})$, the description of which we now turn to.

Theorem 2.7 (The local stable manifold of $\Gamma_1(h)$). *Fix $h \in \left(0, \frac{1}{2}\right)$. Then the stable set $W^s(\Gamma_1(h))$ of $\Gamma_1(h)$ is defined by $H_\infty(r_1, v, l) = h$. Moreover, fix any $k \in \mathbb{N}$. Then there exists a neighboorhood $N(k,h)$ of $\Gamma_1(h)$ such that $W^s_{loc}(\Gamma_1(h)) = W^s(\Gamma_1(h)) \cap N(k,h)$ is a C^k-smooth two-dimensional submanifold. ($W^s_{loc}(\Gamma_1(h))$ is a cylinder). The dependency on h is also C^k-smooth.*

Although the domain $N(k,h)$ depends upon k and h, the flow is regular away from $l = 0$ and we can therefore, as for $W^s_{loc}(q_1)$ above, globalize the local manifolds by application of the backward flow. Moreover, since the system is real analytic, it follows that these global stable manifolds are in fact C^k also. Similarly, if we fix a compact interval $I \subset \left(0, \frac{1}{2}\right)$ then we have a uniform description of all local manifolds within $N(k) := \cap_{h \in I} N(k,h)$ and by working on this set, our approach also shows that the stable manifolds are also C^k, also in $h \in I$. In turn, seeing that $k \in \mathbb{N}$ is arbitrary, we obtain the following:

Theorem 2.8. *The global stable manifolds $W^s(q_1)$ and $W^s(\Gamma_1(h))$ of $q_1 : (r_1, v, l) = (1, 0, 0)$ and $\Gamma_1(h)$, $h \in \left(0, \frac{1}{2}\right)$, respectively, are each C^∞. The dependency of $W^s(\Gamma_1(h))$ on h is also C^∞.*

Due to (2.10), we have obtained a complete description of the smoothness of $|\mathcal{E}_\infty(u, \dot{u})| \in (0,1)$.

Remark 2.9. It seems likely that the global stable manifolds of $\Gamma_1(h)$ are also Gevrey-1 (as the stable manifold $W^s(q_1)$ of $q_1 : (r_1, v, l) = (1, 0, 0)$), but this would require better normal forms. [3] considers related normal forms, but the condition in this paper regarding the trace, implies that q_1 is an attractor (or repeller). This is clearly violated in the present context, but it holds for a more general class of dissipation functions (linear damping is degenerate from this perspective) and in [28] we show that this condition relates directly to the property of circularization.

Finally, we remark that the existence of the invariant set $W^s(q_1)$ was proven more indirectly in [36] using degree theory. Although this approach does not address the smoothness, the result in [37] holds true for a more general class of dissipations defined by $\delta = \delta(|u|)$, with $\delta(|u|) \geqslant c > 0$. However, our results can also be extended to this general case. We leave this to the interested reader.

While the smoothness properties of $W^s(q_1)$ and $W^s(\Gamma_1(h))$ may not have immediate practical applications, it is intriguing that we can apply methods from smooth dynamical systems to examine these objects, that were first identified more indirectly using different methods. At the same time, we again emphasize that our approach is versatile and extends to a broad class of dissipation functions, see [28] where the fundamental issue of circularization is solved for a general class of dissipation functions.

3. Proof of theorem 2.6

To prove theorem 2.6, we consider (2.6) in terms of

$$x = l^3. \tag{3.1}$$

This gives

$$\begin{aligned} r_1' &= v + 2\delta r_1 x, \\ v' &= -\frac{r_1 - 1}{r_1^3} - 2\delta v x, \\ x' &= -3\delta x^2, \end{aligned} \tag{3.2}$$

or

$$\begin{aligned} x^2 \frac{dr_1}{dx} &= \frac{1}{3\delta}\left(-v - 2\delta r_1 x\right), \\ x^2 \frac{dv}{dx} &= \frac{1}{3\delta}\left(\frac{r_1 - 1}{r_1^3} + 2\delta v x\right), \end{aligned} \tag{3.3}$$

upon eliminating time. To zoom in on q_1 at $r_1 = 1, v = 0, x = 0$, we perform a blowup transformation:

$$(x, r_{11}, v_{11}) \mapsto \begin{cases} r_1 &= 1 + x r_{11}, \\ v &= x\left(v_{11} - 2\delta\right), \end{cases} \tag{3.4}$$

leaving x fixed. This gives the final system:

$$x^2 \frac{dy}{dx} = Ay + f(x, y), \tag{3.5}$$

setting $y = (r_{11}, v_{11})$ and where

$$\begin{aligned} A &= \begin{pmatrix} 0 & -\frac{1}{3\delta} \\ \frac{1}{3\delta} & 0 \end{pmatrix}, \\ f(x, r_{11}, v_{11}) &= \frac{1}{3} x \begin{pmatrix} -5\delta^{-1} r_{11} \\ 2\delta - v_{11} - \delta^{-1} r_{11}^2 \left(3 + 3x r_{11} + x^2 r_{11}^2\right)\left(1 + x r_{11}\right)^{-3} \end{pmatrix}. \end{aligned}$$

The eigenvalues of A are $\pm \frac{i}{\sqrt{3\delta}}$ and f is real analytic. It is standard, that there exists a formal series solution

$$y(x) = \widehat{Y}(x) := \sum_{x=1}^{\infty} Y_n x^n, \tag{3.6}$$

of (3.5), see e.g. [4] and also [19] for the details of the expansion in the present case. In particular,

$$Y_1 = \begin{pmatrix} -2\delta^2 \\ 0 \end{pmatrix}, \quad Y_2 = \begin{pmatrix} 0 \\ 16\delta^3 \end{pmatrix},$$

and by induction on n it can be shown that

$$Y_{2n-1} = \begin{pmatrix} * \\ 0 \end{pmatrix}, \quad Y_{2n} = \begin{pmatrix} 0 \\ * \end{pmatrix}, \tag{3.7}$$

for all $n \in \mathbb{N}$. Here $*$ is an unspecified quantity that depends upon n and δ.

Let $S(\phi, r) \subset \mathbb{C}$ be the open sector region in $\mathbb{C}$ centered along the positive real axis, with radius r and opening ϕ:

$$S(\phi, r) = \{x \in \mathbb{C} : |\arg(x)| < \phi/2, 0 < |x| < r\}.$$

Let $\overline{S}(\phi, r)$ denote its closure. The following result shows that the series (3.6) is Gevrey-1 and *1-summable* [2]:

Proposition 3.1. *There exists $x_0 > 0$, $\phi > 0$ both sufficiently small and a Gevrey-1 function $Y : \overline{S}(\phi + \pi, r) \to \mathbb{C}$ with $Y(0) = 0$, which is real analytic on $S(\phi + \pi, r)$, such that the graph*

$$y = Y(x), \quad x \in S(\phi + \pi, r)$$

solves (3.5) with $Y(0) = 0$. Here Y has $\widehat{Y}$, see (3.6), as a Gevrey-1 asymptotic series, such that $Y^{(n)}(0) = n! Y_n$, $Y_n \leqslant ab^n n!$ for $a > 0, b > 0$.

Proof. The result follows from [4, theorem 3]; although this result does not address the existence of an invariant manifold directly (instead [4] proves existence of a certain normal form), this can be obtained as a corollary, using the invariance of the set $y = 0$ of [4, equation (8)]. For completeness, we include a version of the proof that only addresses the existence of $y = Y(x)$, see also [30, appendix], which includes a similar proof.

Following [4] we proceed by first (a) transforming (3.3) into an equation on the 'Borel-plane' (through the Borel-transform $\mathcal{B}$), then (b) apply a fixed-point argument there and finally (c) obtain our desired solution by applying the Laplace transform.

For our purposes, the Borel transform is defined in the following way: If $h(x) = \sum_{n=1}^{\infty} h_n x^n$ is a Gevrey-1 formal series:

$$|h_n| \leqslant ab^n n! \quad a > 0, b > 0, \tag{3.8}$$

then the Borel transform of h is given by

$$\mathcal{B}(h)(u) = \sum_{n=0}^{\infty} \frac{h_{n+1}}{n!} u^n.$$

Clearly, $\mathcal{B}(h)$ is analytic on $|u| < b^{-1}$ if (3.8) holds true. For the Laplace transform, on the other hand, we need analytic functions $\alpha(u)$ that are at most exponentially growing $|\alpha(u)| \leqslant \mathcal{O}(1) e^{\zeta |u|}$, $\zeta > 0$, in an infinite sector. With this in mind, let $S(\phi) \subset \mathbb{C}$ be the (infinite) sector centered along the positive real x-axis with opening $\phi \in (0, \pi)$, and let $B(R)$ be the open ball of radius R centered at 0. Finally, set

$$\Delta := S(\phi) \cup B(R).$$

Then for any $\zeta > 0$, we define the norm

$$\|\alpha\|_\zeta := \sup_{u \in \Delta} \left\{ |\alpha(u)| \left(1 + \zeta^2 |u|^2\right) e^{-\zeta |u|} \right\}, \tag{3.9}$$

see [4], on the space of analytic functions on Δ:

$$\mathcal{G} := \{\alpha : \alpha \text{is analytic on } \Delta \text{and } \|\alpha\|_\zeta < \infty\}.$$

The normed space $(\mathcal{G}, \|\cdot\|_\zeta)$ is a complete space. We will need ζ sufficiently large in the following. The factor $1+\zeta^2|w|^2$ in the norm $\|\cdot\|_\zeta$ ensures that the convolution:

$$(\alpha \star \beta)(u) = \int_0^u \alpha(s)\beta(u-s)\,ds,$$

is continuous as a bilinear operator on $\mathcal{G}$. In particular, we have

$$\|\alpha \star \beta\|_\zeta \leqslant \frac{4\pi}{\zeta}\|\alpha\|_\zeta \|\beta\|_\zeta,$$

see [4, proposition 4]. The Laplace transform (along the positive real axis)

$$\mathcal{L}(\alpha)(x) := \int_0^\infty \alpha(u)\, e^{-u/x} du,$$

is then well-defined for any $\alpha \in \mathcal{G}$. In fact, we have the following result.

Lemma 3.2. [4, *proposition 3*] *The Laplace transform defines a linear continuous mapping, with operator norm* $\|\mathcal{L}\| \leqslant 1$, *from* $\mathcal{G}$ *to the set of analytic functions on a local sector* $S(\pi+\phi, R_0) = S(\pi+\phi) \cap B(R_0)$ *for* $\phi \in (0,\pi)$ *and* $R_0 > 0$ *sufficiently small. Moreover,*

$$\mathcal{L}(\alpha \star \beta)(x) = \mathcal{L}(\alpha)(x)\,\mathcal{L}(\beta)(x),$$

and

$$x^2 \frac{d}{dx}\mathcal{L}(\alpha)(x) = \mathcal{L}(u\alpha)(x), \tag{3.10}$$

with $u\alpha$ *being the function* $u \mapsto u\alpha(u)$, *for every* $\alpha, \beta \in \mathcal{G}$.

Following (3.10), we are now led to write the left hand side of (3.5) with $y = Y(x)$ as $[uI - A]\Phi(u)$ with $\Phi = \mathcal{B}(Y)$. To set up the associated right hand side, we need to deal with the nonlinearity $f(x, Y(x))$. This is described in [4, proposition 5]:

Lemma 3.3. *Write* f *as the convergent series* $f(x,y) = \sum_{n=1}^\infty f_n(x)y^n$, $f_n(x) := \sum_{m=1}^\infty f_{mn}x^m$ *and let* F_n *be the Borel transform of* f_n. *Then* $F_n \in \mathcal{G}$ *for each* n. *Fix* $C_0 > 0$ *and for large values of* ζ, *recall (3.9), consider* $\alpha \in \mathcal{G}$ *with* $\|\alpha\|_\zeta \leqslant C_0$. *Then* $\alpha \mapsto f^*(\alpha)$ *defined by*

$$f^*(\alpha)(u) := \sum_{n=1}^\infty F_n(u) \star \alpha(u)^{\star n},$$

which converges in $\mathcal{G}$, *is differentiable and satisfies the following estimates*

$$\|f^*(\alpha)\|_\zeta \leqslant C_1, \quad \|D(f^*)(\alpha)\|_\zeta \leqslant \zeta^{-1}C_1, \tag{3.11}$$

for some constant $C_1 > 0$ *depending only on* f *and* C_0. *Moreover,*

$$\mathcal{L}(f^*(\alpha))(x) = f(x, \mathcal{L}(\alpha)(x)). \tag{3.12}$$

Following (3.12), we are therefore finally led to consider

$$\Phi(u) = [uI - A]^{-1} f^*(\Phi)(u), \tag{3.13}$$

where Φ is the Borel transform of Y. The equation (3.13) has the form of a fixed point equation. Since the eigenvalues of A are imaginary, if we take $\phi \in (0,\pi)$ then $[uI-A]^{-1}$ is uniformly bounded on $S(\phi)$. Using (3.11), it therefore follows that there is some $M>0$, depending on f, ϕ and R, such that the right hand side of (3.13) defines a contraction on the subset of $\mathcal{G}$ with $\|\cdot\|_\zeta \leqslant M$ for $\zeta > 0$ large enough. Consequently, by Banach's fixed point theorem there is a unique solution $\Phi \in \mathcal{G}, \|\Phi\|_\zeta \leqslant M$, solving (3.13). By applying the Laplace transform, we obtain the desired solution

$$Y(x) := \mathcal{L}(\Phi)(x),$$

of (3.5), using (3.10) and (3.12). The function Y is defined on the domain $S(\pi+\phi, R_0) = S(\pi+\phi) \cap B(R_0)$ and has the properties specified by lemma 3.2. Finally, we emphasize that the Borel transform is real when the argument is. Consequently, (3.13) is real when Φ is real. Since the Laplace transformation is real upon integrating along the positive real axis, $Y = \mathcal{L}(\Phi)$ is real analytic on $S(\pi+\theta, R_0)$ as claimed. □

Upon transforming the manifold in proposition 3.1 back to the (r_1, v, l)-coordinates, using (3.1) and

$$\begin{pmatrix} F_1(l^3) \\ G_1(l^3) + 2\delta \end{pmatrix} := Y(l^3),$$

cf (3.4), we obtain (2.11). Equation (2.12) then also follows from (3.7). The manifold $W^s_{loc}(q_1)$ cannot contain points not in (2.11); this follows from the proof of theorem 2.7, see lemma 4.1. This completes the proof of theorem 2.6.

4. Proof of theorem 2.7

To prove theorem 2.7, we will proceed in three steps: First we introduce appropriate (energy-angle) coordinates to parameterize $H(r_1, v) = h$, see section 4.1. Subsequently in section 4.2, we bring our system into a normal form (based upon averaging). Finally in section 4.3, we use the normal form to set up an equation for the invariant manifold $W^s(\Gamma_1(h))$, which we solve using the implicit function theorem. Essentially, our approach is reminiscent of a flow-box argument; we will show that there are smooth coordinates (h, ϕ, l), $\phi \in \mathbb{T} = \mathbb{R}/(2\pi\mathbb{Z})$, with $h' = 0$.

4.1. Energy-angle coordinates

We first consider the planar Hamiltonian system (2.7), repeated here for convenience:

$$\begin{aligned} r_1' &= v, \\ v' &= -\frac{r_1 - 1}{r_1^3}, \end{aligned} \tag{4.1}$$

with Hamiltonian function:

$$H(r_1, v) = \frac{1}{2}v^2 + \frac{(r_1-1)^2}{2r_1^2}. \tag{4.2}$$

The set $H^{-1}(I)$ with $I := \left(0, \frac{1}{2}\right)$ is filled with periodic orbits $\Gamma_1(h)$ surrounding the point $(r_1, v) = (1, 0)$.

In the following, we write the energy h as H; we believe it should be clear from the context whether H is treated as a variable $H \in I$ or as the function (4.2). Therefore let $(\underline{r}_1(t,H), \underline{v}(t,H))$ denote the solution corresponding to $\Gamma_1(H)$, $H \in I$, satisfying $\underline{r}_1(0,H) = 1, \underline{v}(0,H) > 0$ and denote the minimal period by $p(H) > 0$. Let

$$\underline{t}(H, \phi_1) := (2\pi)^{-1} p(H) \phi_1.$$

Then we consider the following mapping

$$(H, \phi_1) \mapsto \begin{pmatrix} \underline{r}_1(\underline{t}(H, \phi_1), H) \\ \underline{v}(\underline{t}(H, \phi_1), H) \end{pmatrix}, \tag{4.3}$$

from $I \times \mathbb{T}$, $\mathbb{T} := \mathbb{R}/\{2\pi\mathbb{Z}\}$, to the set $H^{-1}(I)$. This mapping is a real-analytic diffeomorphism. In particular, its inverse:

$$\Phi : (r_1, v) \mapsto (H, \phi_1), \tag{4.4}$$

transforms (4.1) into

$$\begin{aligned} H' &= 0, \\ \phi_1' &= \Omega_0(H), \end{aligned}$$

with

$$\Omega_0(H) := \frac{2\pi}{p(H)} > 0. \tag{4.5}$$

We now turn our attention to the $l > 0$-system. We will again prefer to work with $x = l^3$ rather than l and therefore consider (3.2), repeated here for convenience

$$\begin{aligned} r_1' &= v + 2\delta r_1 x, \\ v' &= -\frac{r_1 - 1}{r_1^3} - 2\delta v x, \\ x' &= -3\delta x^2. \end{aligned} \tag{4.6}$$

Lemma 4.1. *Let X_1 denote the vector-field of (4.6) and define the following function*

$$H_1(r_1, v, x) := H(r_1, v) + 2\delta r_1 v x + 3\delta^2 r_1^2 x^2.$$

Then

$$\mathcal{L}_{X_1} H_1(r_1, v, x) = -6\delta^3 r_1^2 x^3, \tag{4.7}$$

where $\mathcal{L}_{X_1} H_1 = \nabla H_1 \cdot X_1$ is the Lie-derivative.

Proof. Follows from a direct calculation:

$$\frac{\partial H_1}{\partial r_1} r_1' + \frac{\partial H_1}{\partial v} v' = 6\delta^2 r_1 v x^2 + 12\delta^3 r_1 x^3, \quad \frac{\partial H_1}{\partial x} x' = -6\delta^2 r_1 v x^2 - 18\delta^3 r_1^2 x^3,$$

so that

$$\mathcal{L}_{X_1} H_1 = \frac{\partial H_1}{\partial r_1} r_1' + \frac{\partial H_1}{\partial v} v' + \frac{\partial H_1}{\partial x} x' = -6\delta^3 r_1^2 x^3.$$

□

We proceed to use (H_1, ϕ_1, x) as coordinates.

Lemma 4.2. *Fix an open interval J such that $\bar{J} \subset I$. Then there exists an $x_0 > 0$ such that*

$$\widetilde{\Psi} : (r_1, v, x) \mapsto (H_1, \phi_1, x)$$

defined on $H^{-1}(J) \times (-x_0, x_0)$, is a real analytic diffeomorphism.

Proof. The mapping $\widetilde{\Psi}(r_1, v, x) = (\widetilde{\Psi}_1(r_1, v, x), \widetilde{\Psi}_2(r_1, v, x), x)$ is an x-fibered (polynomial) perturbation of the cartesian product of diffeomorphisms $(r_1, v) \mapsto (\Phi_1(r_1, v), \Phi_2(r_1, v))$, $x \mapsto x$, recall (4.4). The result therefore follows by the inverse function theorem. □

Lemma 4.3. *Let X_1 denote the vector-field of (4.6) and consider $\widetilde{\Psi}$ from lemma 4.2. Then $\widetilde{\Psi}_* X_1$ takes the following form:*

$$\begin{aligned} H_1' &= x^3 R_1(H_1, \phi_1, x), \\ \phi_1' &= \Omega_0(H_1) + x P_1(H_1, \phi_1, x), \\ x' &= -3\delta x^2, \end{aligned} \tag{4.8}$$

for all $H_1 \in J$. The functions R_1 and P_1 are both real-analytic functions defined on $J \times \mathbb{T} \times (-x_1, x_1)$ for $x_1 > 0$ sufficiently small.

Proof. The result follows directly from (4.5), lemmas 4.1 and 4.2. In particular, by (4.7) we have that

$$R_1(H_1, \phi_1, x) = -6\delta^3 r_1^2,$$

with $r_1 = r_1(H_1, \phi_1, x)$, cf lemma 4.2. □

4.2. A normal form

We will now use an averaging approach to normalize (4.8). This will consist of pushing the angle-dependency to higher order with respect to x.

Lemma 4.4 (The Iterative lemma). *Consider the real-analytic system*

$$\begin{aligned} H_n' &= x^3 \Lambda_n(H_n, x) + x^{n+2} R_n(H_n, \phi_n, x), \\ \phi_n' &= \Omega_n(H_n, x) + x^n P_n(H_n, \phi_n, x), \\ x' &= -3\delta x^2, \end{aligned} \tag{4.9}$$

defined on $J_n \times \mathbb{T} \times (-x_n, x_n)$ and with $n \in \mathbb{N}$. Here $\Omega_n(H_n, 0) = \Omega_0(H_n) \geqslant c > 0$. Then for any $J_{n+1} \subset J_n$ there exists a constant $x_{n+1} > 0$ and an x-fibered, real-analytic diffeomorphism $(H_n, \phi_n, x) \mapsto (H_{n+1}, \phi_{n+}, x)$ of the near-identify form

$$H_{n+1} = H_n + x^{n+2} T_n(H_n, \phi_n, x), \tag{4.10}$$

$$\phi_{n+1} = \phi_n + x^n Q_n(H_n, \phi_n, x), \tag{4.11}$$

such that

$$\begin{aligned} H'_{n+1} &= x^3\Lambda_{n+1}\left(H_{n+1},x\right)+x^{n+3}R_{n+1}\left(H_{n+1},\phi_{n+1},x\right),\\ \phi'_{n+1} &= \Omega_{n+1}\left(H_{n+1},x\right)+x^{n+1}P_{n+1}\left(H_{n+1},\phi_{n+1},x\right),\\ x' &= -3\delta x^2, \end{aligned} \tag{4.12}$$

with the right hand side being real-analytic on $J_{n+1}\times\mathbb{T}\times(-x_{n+1},x_{n+1})$.

Proof. The result follows from a modification of the classical averaging theorem, see e.g. [17]. We write

$$R_n\left(H_n,\phi_n,x\right)=\overline{R}_n\left(H_n,x\right)+\widetilde{R}_n\left(H_n,\phi_n,x\right),$$

where

$$\overline{R}_n\left(H_n,x\right):=\frac{1}{2\pi}\int_0^{2\pi}R_n\left(H_n,s,x\right)ds,$$

is the mean of $\phi\mapsto R_n(H_n,\phi,x)$, and where $\widetilde{R}_n$ has zero mean:

$$\int_0^{2\pi}\widetilde{R}_n\left(H_n,s,x\right)ds=0. \tag{4.13}$$

We then take

$$T_n\left(H_n,\phi_n,x\right):=-\Omega_0\left(H_n\right)^{-1}\int_0^{\phi_n}\widetilde{R}_n\left(H_n,s,x\right)ds,$$

in (4.10). Notice that T_n is well-defined for $\phi_n\in\mathbb{T}$ by (4.13). Moreover,

$$\frac{\partial}{\partial\phi_n}T_n\left(H_n,\phi_n,x\right)=-\Omega_0\left(H_n\right)^{-1}\widetilde{R}_n\left(H_n,\phi_n,x\right). \tag{4.14}$$

We therefore have by (4.10):

$$\begin{aligned} H'_{n+1} &= H'_n+x^{n+2}\frac{\partial}{\partial\phi}T_n\left(H_n,\phi_n,x\right)\phi'_n+\mathcal{O}\left(x^{n+3}\right)\\ &= x^3\Lambda_n\left(H_n,x\right)+x^{n+2}\overline{R}_n\left(H_n,x\right)+x^{n+2}\left\{\widetilde{R}_n\left(H_n,\phi_n,x\right)+\frac{\partial}{\partial\phi_n}T_n\left(H_n,\phi_n,x\right)\Omega_0\left(H_n\right)\right\}\\ &\quad+\mathcal{O}\left(x^{n+3}\right)\\ &:= x^3\Lambda_{n+1}\left(H_{n+1},x\right)+x^{n+3}R_{n+\frac{1}{2}}\left(H_{n+1},\phi_n,x\right), \end{aligned}$$

with

$$\Lambda_{n+1}\left(H_{n+1},x\right):=\Lambda_n\left(H_{n+1},x\right)+x^n\overline{R}_n\left(H_{n+1},x\right),$$

using (4.14) to conclude that $\{\cdots\}=0$.

Subsequently, we define

$$P_{n+\frac{1}{2}}\left(H_{n+1},\phi_n,x\right):=x^{-n}\left[\Omega_n\left(H_n,x\right)-\Omega_n\left(H_{n+1},x\right)+x^nP_n\left(H_n,\phi_n,x\right)\right],$$

such that

$$\phi_n' = \Omega_n\left(H_{n+1},x\right) + x^n P_{n+\frac{1}{2}}\left(H_{n+1},\phi_n,x\right).$$

It follows from (4.10) that $P_{n+\frac{1}{2}}$ extends smoothly to $x=0$. We write

$$P_{n+\frac{1}{2}}\left(H_{n+1},\phi_n,x\right) = \overline{P}_{n+\frac{1}{2}}\left(H_{n+1},x\right) + \widetilde{P}_{n+\frac{1}{2}}\left(H_{n+1},\phi_n,x\right),$$

where

$$\overline{P}_{n+\frac{1}{2}}\left(H_{n+1},x\right) := \frac{1}{2\pi}\int_0^{2\pi} P_{n+\frac{1}{2}}\left(H_{n+1},s,x\right) ds,$$

is the mean of $\phi \mapsto P_{n+\frac{1}{2}}(H_{n+1},\phi,x)$, and where $\widetilde{P}_{n+\frac{1}{2}}$ has zero mean:

$$\int_0^{2\pi} \widetilde{P}_{n+\frac{1}{2}}\left(H_{n+1},s,x\right) ds = 0.$$

Then we apply the same procedure on the ϕ_n-equation. In particular, we consider a transformation defined by

$$\phi_{n+1} = \phi_n + x^n Q_{n+\frac{1}{2}}\left(H_{n+1},\phi_n,x\right),$$

fixing H_{n+1} and x, with

$$Q_{n+\frac{1}{2}}\left(H_{n+1},\phi_n,x\right) := -\Omega_0\left(H_{n+1}\right)^{-1}\int_0^{\phi_n} \widetilde{P}_{n+\frac{1}{2}}\left(H_{n+1},s,x\right) ds. \tag{4.15}$$

This leads to the following equation for ϕ_{n+1}:

$$\begin{aligned}
\phi_{n+1}' &= \phi_n' + x^n \frac{\partial}{\partial \phi_n} Q_{n+\frac{1}{2}}\left(H_{n+1},\phi_n,x\right)\phi_n' + \mathcal{O}\left(x^{n+1}\right)\\
&= \Omega_n\left(H_{n+1},x\right) + x^n \overline{P}_{n+\frac{1}{2}}\left(H_{n+1},x\right)\\
&\quad + x^n\left\{\widetilde{P}_{n+\frac{1}{2}}\left(H_{n+1},\phi,x\right) + \frac{\partial}{\partial \phi_n} Q_{n+\frac{1}{2}}\left(H_{n+1},\phi_n,x\right)\Omega_0\left(H_{n+1}\right)\right\} + \mathcal{O}\left(x^{n+1}\right)\\
&=: \Omega_{n+1}\left(H_{n+1},x\right) + x^{n+1} P_{n+1}\left(H_{n+1},\phi_{n+1},x\right),
\end{aligned}$$

with

$$\Omega_{n+1}\left(H_{n+1},x\right) := \Omega_n\left(H_{n+1},x\right) + x^n \overline{P}_{n+\frac{1}{2}}\left(H_{n+1},x\right),$$

using (4.15) to conclude that $\{\cdots\} = 0$. Finally, we put

$$R_{n+1}\left(H_{n+1},\phi_{n+1},x\right) := R_{n+\frac{1}{2}}\left(H_{n+1},\phi_n,x\right).$$

This completes the proof. □

Since (4.8) satisfies the conditions of The Iterative Lemma with $n=1$ and $\Lambda_1(H_1,x)\equiv 0$, $\Omega_1(H_1,x)\equiv\Omega_0(H_1)$, we conclude that for every $J\subset I$ and every $N\in\mathbb{N}_0$, we can transform (4.8) into 'the normal form':

$$\begin{aligned} H'_{N+1} &= x^3\Lambda_{N+1}\left(H_{N+1},x\right)+x^{N+3}R_{N+1}\left(H_{N+1},\phi_{N+1},x\right),\\ \phi'_{N+1} &= \Omega_{N+1}\left(H_{N+1},x\right)+x^{N+1}P_{N+1}\left(H_{N+1},\phi_{N+1},x\right),\\ x' &= -3\delta x^2, \end{aligned} \tag{4.16}$$

on $J\times\mathbb{T}\times(-x_{N+1},x_{N+1})$ for $x_{N+1}>0$ sufficiently small, by a near-identify transformation of H and ϕ. We drop the subscripts henceforth and write it in the equivalent form

$$\begin{aligned} \frac{dH}{d\tau} &= \frac{1}{3\delta}x\left[\Lambda\left(H,x\right)+x^N R\left(H,\phi,x\right)\right],\\ \frac{d\phi}{d\tau} &= \frac{1}{3\delta x^2}\left\{\Omega\left(H,x\right)+x^{N+1}P\left(H,\phi,x\right)\right\},\\ \frac{dx}{d\tau} &= -1, \end{aligned} \tag{4.17}$$

for $x>0$. Let $\underline{H}(\tau,H_0,\phi_0,x_0),\underline{\phi}(\tau,H_0,\phi_0,x_0),\underline{x}(\tau,H_0,\phi_0,x_0)=x_0-\tau$, satisfying

$$\underline{z}(0,\cdot)=z_0,$$

for $z=H,\phi,x$, denote the flow of (4.17).

Lemma 4.5. *$\underline{H},\underline{\phi}$ and $\underline{x}$ are C^∞ on the set*

$$V(\xi):=\left\{(\tau,H_0,\phi_0,x_0)\in(0,\xi)\times J\times\mathbb{T}\times(0,\xi)\,:\,0<\tau<x_0\right\}, \tag{4.18}$$

for $\xi>0$ sufficiently small.

Proof. The right hand side is smooth, even real-analytic, and the existence of a smooth local flow $\underline{H}(\tau,H_0,\phi_0,x_0),\underline{\phi}(\tau,H_0,\phi_0,x_0),\underline{x}(\tau,H_0,\phi_0,x_0)=x_0-\tau$, with $\tau\in I(H_0,\phi_0,x_0):=(0,\tau_{\max})$, therefore follows. We then integrate both sides of (4.17):

$$\begin{aligned} \underline{H}(\tau,H_0,\phi_0,x_0) &= H_0-\frac{1}{3\delta}\int_{x_0}^{x}s\left[\cdots\right]ds,\\ \underline{\phi}(\tau,\phi_0,x_0) &= \phi_0-\frac{1}{3\delta}\int_{x_0}^{x}s^{-2}\left\{\cdots\right\}ds, \end{aligned} \tag{4.19}$$

with $x=x_0-\tau$, and $[\cdots]$, $\{\cdots\}$ being the brackets in (4.17) evaluated at $H=\underline{H}(x_0-x,H_0,\phi_0,x_0),\phi=\underline{\phi}(x_0-x,H_0,\phi_0,x_0)$. It is then standard to arrive at the following estimate for $\tau\in I(H_0,\phi_0,x_0)$:

$$|\underline{H}(\tau,H_0,\phi_0,x_0)-H_0|\leqslant C|\tau|\leqslant Cx_0,\quad |\underline{\phi}(\tau,H_0,\phi_0,x_0)-\phi_0||\tau-x_0|\leqslant C, \tag{4.20}$$

for some $C>0$ large enough and all $(H_0,\phi_0,x_0)\in J\times\mathbb{T}\times(0,\xi)$, provided that $\xi>0$ is small enough. This shows that $\tau_{\max}=x_0$ and completes the proof. □

4.3. The existence of smooth invariant manifolds

The inequalities in (4.20) provide C^0-estimates of $\underline{H}$ and $\underline{\phi}$, respectively.

Lemma 4.6. *The function $\underline{H}(\tau,H_0,\phi_0,x_0)$ extends continuously to the closure $\overline{V(\xi)}$, recall (4.18), with $\underline{H}(0,H_0,\phi_0,0)=H_0$ for all $(H_0,\phi_0)\in J\times\mathbb{T}$.*

Remark 4.7. This is true even though $\underline{\phi}$ itself does not extend to $\tau=x_0$.

Proof. Consider $\underline{\phi}(\tau,H_0,\phi_0,x_0)$ given for $\tau\in[0,x_0)$. It is continuous on $V(\xi)$. Moreover,

$$(\tau,x_0)\mapsto \underline{H}(\tau,H_0,\phi_0,x_0)\,,$$

is absolutely continuous, uniformly in $(H_0,\phi_0)\in J\times\mathbb{T}$, see (4.19). Consequently, $\underline{H}$ extends continuously and uniquely to the closure $\overline{V(\xi)}$. Moreover, $\underline{H}(0,H_0,\phi_0,x_0)=H_0$ by definition for all $x_0\in(0,\xi)$ and therefore also $\underline{H}(0,H_0,\phi_0,0)=H_0$. □

Let $h\in J_0\subset J$. We then consider the resulting equation

$$h=\underline{H}(x,H,\phi,x)\,, \tag{4.21}$$

with $(H,\phi,x)\mapsto\underline{H}(x,H,\phi,x)$ being defined and continuous by lemma 4.6 on $J\times\mathbb{T}\times[0,\xi]$.

Lemma 4.8. *The equation (4.21) defines an invariant set $W^s(\Gamma_1(h))$ in the (H,ϕ,x)-space.*

Proof. $(x_0,H_0,\phi_0)\in W^s(\Gamma_1(h))\Longrightarrow$

$$\begin{aligned}h&=\lim_{\tau\to x_0^-}\underline{H}(\tau,H_0,\phi_0,x_0)\\&=\lim_{\tau\to(x_0-s)^-}\underline{H}\left(\tau,\underline{H}(s,H_0,\phi_0,x_0),\underline{\phi}(s,H_0,\phi_0,x_0),x_0-s\right)\\&=\underline{H}\left(x_0-s,\underline{H}(s,H_0,\phi_0,x_0),\underline{\phi}(s,H_0,\phi_0,x_0),x_0-s\right),\end{aligned}$$

using the group properties of the flow. Consequently, $(\underline{H}(s,H_0,\phi_0,x_0),\underline{\phi}(s,H_0,\phi_0,x_0),x_0-s)\in W^s(\Gamma_1(h))$ for all $s\in(0,x_0)$. □

In terms of the time s (say) used in (4.16), $\tau\to x_0^-$ corresponds to $s\to\infty$. Then by (a):

$$\underline{H}(0,H_0,\phi_0,0)=\frac{1}{2}v^2+\frac{(r_1-1)^2}{2r_1^2},$$

recall (2.8), see also lemmas 4.2 and 4.4, and (b): the extension of $\underline{H}$ in lemma 4.6 is unique, we conclude that $W^s(\Gamma_1(h))$ is the stable set of $\Gamma_1(h)$, $h\in J_0\subset(0,\frac{1}{2})$, as desired.

Proposition 4.9. *Consider (4.17) with $N\in\mathbb{N}$ fixed and suppose that there is an $M\in\mathbb{N}$ so that $\underline{H}$ extends as a C^M-smooth function to the closure $\overline{V(\xi)}$, recall (4.18), satisfying*

$$\frac{\partial}{\partial H_0}\underline{H}(0,H_0,\phi_0,0)=1. \tag{4.22}$$

Then for any $J_0\subset J$ there exists a $\xi>0$ such that the following holds:

The equation (4.21) with $h\in J_0$ has a unique solution for $(H,\phi,x)\in J\times\mathbb{T}\times[0,\xi]$ of the following graph form

$$H=F(h,\phi,x)\,, \tag{4.23}$$

with $F\in C^M$ on $J_0\times\mathbb{T}\times[0,\xi]$.

Proof. Follows directly from the implicit function theorem. Indeed, we have

$$h = \underline{H}(0,h,\phi,0)\,, \quad \frac{\partial}{\partial H_0}\underline{H}(0,h,\phi,0) = 1,$$

for all $\phi \in \mathbb{T}$ by (4.22), and the right hand side of (4.21) is well-defined and C^M with respect to $(H,\phi,x) \in J \times \mathbb{T} \times [0,x_0]$ by assumption. Consequently, we can solve (4.21) for H as a function of h,ϕ,x. This gives (4.23) and F is C^M-smooth since $\underline{H}$ is so. □

Under the assumptions of proposition 4.9, we then have the following by returning to $l = x^3$: For any $h \in J_0$, (4.23) parametrizes $W^s(\Gamma_1(h))$ locally in the (H,ϕ,l)-space as a C^M-smooth graph $H = F(h,\phi,l^3)$, $\phi \in \mathbb{T}$, $l \in (0,\xi^{1/3})$. Now, by lemmas 4.2 and 4.4, it follows that $(r_1,v,l) \mapsto (H,\phi,l)$, with $l \in (0,\xi^{1/3})$ for $\xi > 0$ small enough, is a smooth diffeomorphism (on the relevant set). Therefore we obtain a C^M invariant manifold $W^s(\Gamma_1(h))$ as the stable set of $\Gamma_1(h)$ in the original (r_1,v,l)-space, as desired.

Consequently, in order to finish the proof of theorem 2.7, it suffices to verify the conditions of proposition 4.9 and to note that M can be taken to be arbitrary (upon increasing N). We will show that we can take $M = \lfloor \frac{N}{2} \rfloor$. Here $\lfloor x \rfloor$ for $x \in \mathbb{R}$ is the floor function, i.e. $n = \lfloor x \rfloor$ is the largest integer such that $n \leqslant x$. The function $\underline{H}$ clearly satisfies (4.22) once we have shown that it extends C^M-smoothly to $\overline{V(\xi)}$.

Define

$$\underline{z}_\nu := \frac{\partial^{|\nu|}}{\partial \tau^{\nu_1} \partial H_0^{\nu_2} \partial \phi_0^{\nu_3} \partial x_0^{\nu_4}} \underline{z}, \tag{4.24}$$

for $z = H,\phi,x$ and where $\nu = (\nu_1,\nu_2,\nu_3,\nu_3) \in \mathbb{N}_0^4$, $|\nu| = \nu_1 + \cdots + \nu_4 \geqslant 0$.

Lemma 4.10. *Fix any $N \in \mathbb{N}$ with $N \geqslant 3$ and let $M = \lfloor \frac{N}{2} \rfloor$. Then there exists a constant $C_N > 0$ large enough, and a constant $\xi > 0$ small enough such that*

$$|\underline{H}_\nu(\tau,H_0,\phi_0,x_0)| \leqslant C_N,$$

for $(\tau,H_0,\phi_0,x_0) \in \overline{V(\xi)}$, and all $|\nu| \leqslant M$.

Proof. The proof is delayed to the appendix. It rests upon careful estimation of the higher order variational equation of (4.17). The main difficulty lies in estimating $\underline{\phi}_\nu$, due to the singular nature of (4.17) at $x = 0$. We find that

$$|\underline{\phi}_\nu(\tau,H_0,\phi_0,x_0)|\,|\tau - x_0|^{1+\nu_1+\nu_4} \leqslant C_N,$$

for $(\tau,H_0,\phi_0,x_0) \in V(\xi)$, and all $|\nu| \leqslant M$. Upon using that the ϕ-dependent term in the H-equation has a x^{N+1}-factor, this allow us to control and extend (as in the proof of lemma 4.6) $\underline{H}_\nu$ to the closure $\overline{V(\xi)}$ provided that $N > \nu_1 + \nu_4$. □

5. Blowing up the linearly damped Kepler problem

In section 2, we characterized constant values of $|\mathcal{E}_\infty| \in (0,1)$ as a smooth cylinder in the (r_1,v,l)-space, see theorem 2.7. The set defined by $\mathcal{E}_\infty = 0$, on the other hand, became a one-dimensional manifold, see theorem 2.6. At the same time, since $|\mathcal{E}_\infty| = 1 \Rightarrow L = 0$, see [36], $|\mathcal{E}_\infty| = 1$ is the plane defined by $(r,v,0)$ in the (r,v,l)-space. Here $|\mathcal{E}_\infty| = 0$ and $|\mathcal{E}_\infty| = 1$ are therefore special cases where the associated invariant sets bifurcate. From [36, 37], it is also

known that $|\mathcal{E}_\infty| \in [0,1]$ and that all values are attained in this set. In our characterization of $|\mathcal{E}_\infty|$ through the Hamiltonian function H, see (2.9) and (2.10), this means the following:

Lemma 5.1. *The set $\Gamma_1(h)$ defined by $H(r_1,v) = h, \rho_1 = 0$ with $h \geqslant \frac{1}{2}$, is not an ω-limit set.*

Proof. $H(r_1,v) > \frac{1}{2}$ is obvious since then $|\mathcal{E}_\infty| > 1$, which would contradict [36]. Moreover, although $H(r_1,v) = \frac{1}{2}$ corresponds to $|\mathcal{E}_\infty| = 1$ it cannot be an ω-limit set either, because of $|\mathcal{E}_\infty| = 1 \Rightarrow L = 0$, cf [36], which is an invariant set (that does not contain $\Gamma_1(h)$). □

We obtained this result as a corollary of [36]. It cannot be understood directly from the perspective in section 2. However, in this section, we will perform a thorough geometric description of the dynamics of (1.1) within the orbital plane, i.e. $u = re^{i\theta}$, by using the blowup method (as well as desingularization and compactification). In this way, we obtain a system where all singularities have associated eigenvalues with nonzero real part (with the exception of q which only has imaginary eigenvalues), and this allows us to interpret lemma 5.1 in a separate geometric way, which will also shed light on $|\mathcal{E}_\infty| \to 1$ (corresponding to $h \to \frac{1}{2}$ cf (2.10)), see also section 6. In future work, we will apply a similar blowup for the description of (1.1) for more general nonlinear dissipation functions where $\delta = \delta(u,\dot{u})$, see also [28].

Our starting point for our blowup approach is to use the coordinates (r,v,l), recall (2.4) and (2.2). This produces the following system

$$\begin{aligned} \dot{r} &= \frac{v}{l}, \\ \dot{v} &= \frac{l^3}{r^3} - \frac{l}{r^2} - 2\delta v, \\ \dot{l} &= -\delta l. \end{aligned} \tag{5.1}$$

We now define a reparametrization of time, corresponding to multiplication of the right hand side of (5.1) by lr^3:

$$\begin{aligned} r' &= vr^3, \\ v' &= l\left(l^3 - rl - 2\delta r^3 v\right), \\ l' &= -\delta r^3 l^2. \end{aligned} \tag{5.2}$$

(5.1) and (5.2) are equivalent for $r > 0$, $l > 0$, but (5.2) has the advantage of being well-defined on $r = 0, l = 0$. This enables the use of dynamical systems theory to infer properties from $r = 0, l = 0$, to $r > 0, l > 0$ for (5.2) and therefore also (5.1).

The system (5.2) has two invariant planes: $\{r = 0\}$ where

$$\begin{aligned} v' &= l^4, \\ l' &= 0, \end{aligned}$$

and $\{l = 0\}$ where

$$\begin{aligned} r' &= vr^3, \\ v' &= 0, \end{aligned}$$

see figure 3. Their intersection $V = \{r = l = 0\}$ and $P = \{v = l = 0\}$ consist entirely of completely degenerate equilibria $v' = 0$, insofar that the linearization about any point in V or P has only zero eigenvalues. We therefore apply the blowup method, see [14, 15]. We

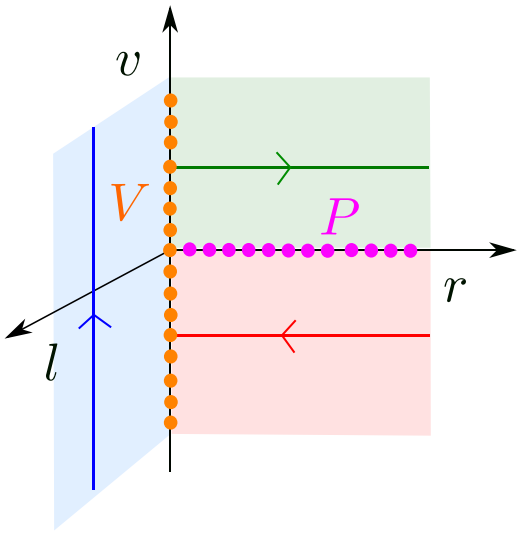

Figure 3. Dynamics of (5.2). The sets V and P are degenerate equilibria.

proceed as follows: First, we blow up V by application of the following cylindrical blowup transformation

$$\Phi^V: \quad \rho \geqslant 0, (\bar{r}, \bar{l}) \in S^1 \mapsto \begin{cases} r &= \rho^2 \bar{r}, \\ l &= \rho \bar{l}, \end{cases} \tag{5.3}$$

which fixes v. See figure 4. Let X denote the vector-field in (5.2). Then the blowup weights are chosen so that $\overline{X} = \Phi^V_* X$ has ρ^4 as a common factor. It is therefore the desingularized vector-field $\rho^{-4}\overline{X}$, that we study in the following. To perform calculations, we work in two separate charts, that we will denote by $(\bar{l}=1)_1$ and $(\bar{r}=1)_2$, respectively, with chart-specific coordinates (r_1, v, ρ_1) and (ρ_2, v, l_2) defined by

$$(\bar{l}=1)_1: \quad \begin{cases} r &= \rho_1^2 r_1, \\ l &= \rho_1, \end{cases} \tag{5.4}$$

$$(\bar{r}=1)_2: \quad \begin{cases} r &= \rho_2^2, \\ l &= \rho_2 l_2. \end{cases} \tag{5.5}$$

See also figure 4 for an illustration of these coordinates. The following expressions

$$\rho_2 = \rho_1 \sqrt{r_1}, \quad l_2 = 1/\sqrt{r_1},$$

define the smooth change of coordinates for $\rho_1 \geqslant 0, r_1 > 0$. We will achieve the desingularization through division of the local vector-fields by ρ_1^4 and ρ_2^4, respectively.

Remark 5.2. We used the r_1-coordinate of (5.4) in section 2, see (2.4), to prove theorem 2.6 and theorem 2.7. The coordinates in the $(\bar{r}=1)_2$-chart allow us to follow and analyze the unbounded orbits $\Gamma(h)$ for $h \geqslant \frac{1}{2}$.

Subsequently, in the $(\bar{r}=1)_2$-chart, we will find that the set P_2 defined by

$$v_2 = 0, l_2 = 0,$$

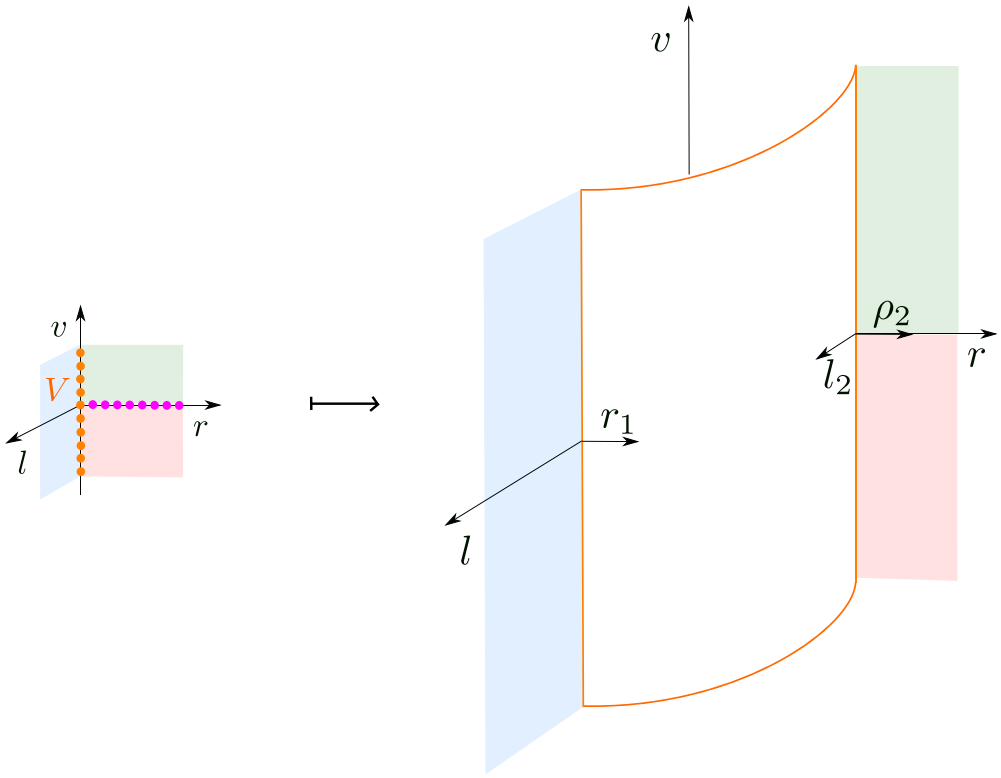

Figure 4. Illustration of the cylindrical blowup of the degenerate set V, see (5.3).

and $\rho_2 \geqslant 0$, is a set of completely degenerate equilibria; this set clearly corresponds to P. We therefore blowup P_2 by application of the following cylindrical blowup transformation:

$$\Phi^{P_2}: \quad \mu \geqslant 0, (\bar{v}, \bar{l}_2) \in S^1 \mapsto \begin{cases} v &= \mu\bar{v}, \\ l &= \mu\bar{l}_2, \end{cases} \tag{5.6}$$

leaving ρ_2 fixed. See figure 5. Let X_2 denote the local vector-field in the $(\bar{r}=1)_2$-chart. Then $\overline{X}_2 = \Phi_*^{P_2} X_2$ has μ as a common factor. It is therefore the desingularized vector-field $\mu^{-1}\overline{X}_2$, that we study in the following. To perform calculations, we work in three separate charts $(\bar{r}=1, \bar{l}_2=1)_{21}$, $(\bar{r}=1, \bar{v}=1)_{22}$ and $(\bar{r}=1, \bar{v}=-1)_{23}$ with chart-specific coordinates (ρ_2, v_1, μ_1), (ρ_2, μ_2, l_{22}) and (ρ_2, μ_3, l_{23}) defined by

$$(\bar{r}=1, \bar{l}_2=1)_{21}: \quad \begin{cases} v &= \mu_1 v_1, \\ l_2 &= \mu_1, \end{cases} \tag{5.7}$$

$$(\bar{r}=1, \bar{v}=1)_{22}: \quad \begin{cases} v &= \mu_2, \\ l_2 &= \mu_2 l_{22}, \end{cases} \tag{5.8}$$

$$(\bar{r}=1, \bar{v}=-1)_{23}: \quad \begin{cases} v &= -\mu_3, \\ l_2 &= \mu_3 l_{23}. \end{cases} \tag{5.9}$$

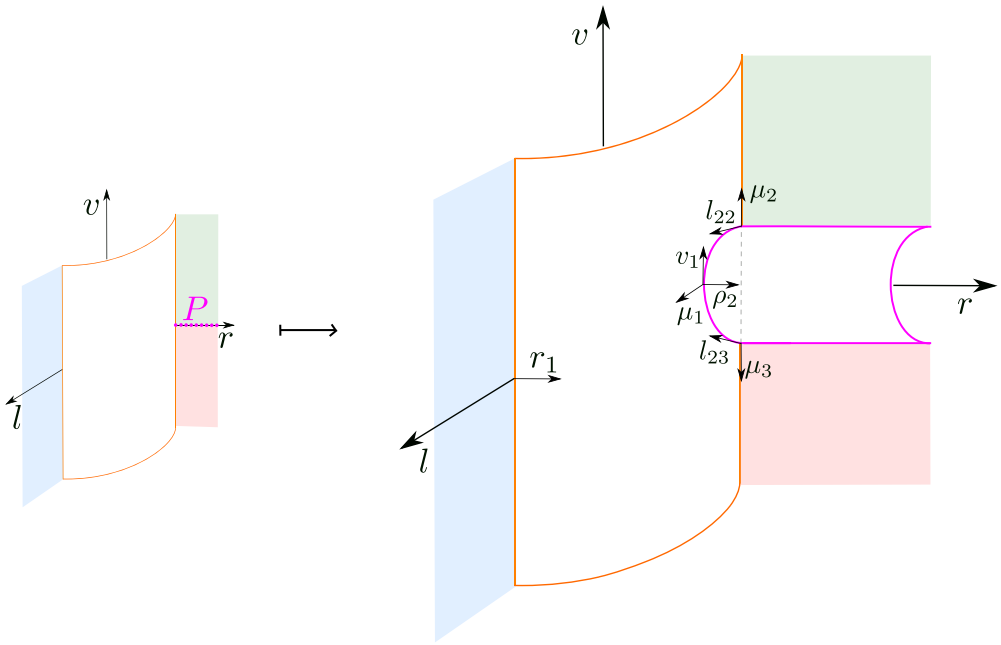

Figure 5. Illustration of the cylindrical blowup of the degenerate set P_2, see (5.6).

See also figure 5 for an illustration of these coordinates. The change of coordinates between $(\bar{r}=1,\bar{l}_2=1)_{21}$ and $(\bar{r}=1,\bar{v}=1)_{22}$ is given by

$$\mu_2=\mu_1 v_1,\quad l_{22}=v_1^{-1}, \tag{5.10}$$

for $\mu_1\geqslant 0$, $v_1>0$. Similarly, between $(\bar{r}=1,\bar{l}_2=1)_{21}$ and $(\bar{r}=1,\bar{v}=-1)_{22}$ we have

$$\mu_3=\mu_1(-v_1),\quad l_{23}=-v_1^{-1}, \tag{5.11}$$

for $v_1<0$. We will achieve the desingularization in each of the charts through division of the local vector-fields by μ_i, $i=1,2,3$, respectively.

Remark 5.3. Using (5.5) and (2.4), we have that v_1 in (5.7) can be written in terms of r and $\dot{r}$ as follows:

$$v_1=\rho_2\dot{r}. \tag{5.12}$$

The equations, we obtain in the $(\bar{r}=1,\bar{l}_2=1)_{21}$-chart, see section 5.3 and (5.19), are therefore equivalent to (2.3) on $r=\rho_2^2>0$. However, the factor of ρ_2 in (5.12) induces a compactification of $\dot{r}$. See also remark 5.6.

As we will see, orbits in $(\bar{r}=1,\bar{v}=1)_{22}$ go unbounded (with $\rho_2\to\infty$). We will therefore need to compactify the space (ρ_1,μ_2,l_{22}). It turns out that the most convenient way to do this is as follows:

$$(\nu, l_{222}) \mapsto \begin{cases} \rho_2 & = \nu^{-1}, \\ l_{22} & = \nu^3 l_{222}, \end{cases} \tag{5.13}$$

with $\nu \geqslant 0, l_{222} \geqslant 0$, leaving μ_2 fixed. In this way, $\nu = 0$ corresponds to $\rho_2 = \infty$ (or $r = \infty$ by (5.4)) and $l_{22} = 0$. The latter property may seem unnatural, but upon using (5.10), we may realize that it leads to the following compactification of the (ρ_2, v_1, μ_1)-space associated with the $(\bar{r} = 1, \bar{l}_2 = 1)_{21}$-chart:

$$(\nu, v_{11}) \mapsto \begin{cases} \rho_2 & = \nu^{-1}, \\ v_1 & = \nu^{-3} v_{11}, \\ \mu_1 & = \nu^3 \mu_{11} \end{cases} \tag{5.14}$$

where $v_{11} = l_{222}^{-1}$, $\mu_{11} = \mu_2 l_{222}$. Using (5.11), we then also obtain the following compactification in the $(\bar{r} = 1, \bar{v} = -1)_{23}$-chart:

$$(\nu, l_{23}) \mapsto \begin{cases} \rho_2 & = \nu^{-1}, \\ l_{23} & = \nu^3 l_{233} \end{cases} \tag{5.15}$$

with $\nu \geqslant 0, l_{233} \geqslant 0$, leaving μ_3 fixed.

We present the final geometric picture of our compactified phase space in a schematic way in figure 6. This figure also illustrates the coordinates used at $r = \infty$.

In the following section, we study the dynamics in each of the charts.

Remark 5.4. In fairness, orbits within $\{r = 0\}$ are also unbounded in the v-direction for $l > 0$, see figure 3, and from this perspective, it is also desirable to compactify the v-direction. However, for simplicity we have chosen not to include this.

5.1. *Chart* $(\bar{l} = 1)_1$

By inserting (5.4) into (5.2), we obtain

$$\begin{aligned} r_1' &= v r_1^3 + 2\delta r_1^4 \rho_1^3, \\ v' &= -r_1 + 1 - 2\delta v r_1^3 \rho_1^3, \\ \rho_1' &= -\delta r_1^3 \rho_1^4, \end{aligned} \tag{5.16}$$

after desingularization, corresponding to division of the right hand side by ρ_1^4. Setting $\rho_1 = l$ and dividing the right hand side by r_1^3, we obtain (2.6). Consequently, within $\rho_1 = 0$, we have the Hamiltonian system with Hamiltonian function $H(r_1, v) = \frac{1}{2} v^2 + \frac{(r_1 - 1)^2}{2 r_1^2}$, recall (2.8), having periodic orbits $\Gamma_1(h)$, $h \in \left(0, \frac{1}{2}\right)$ within $\rho_1 = 0$, surrounding the center $(r_1, v) = (1, 0)$. Theorems 2.6 and 2.7 gave the existence of stable manifolds of $(r_1, v, \rho_1) = (1, 0, 0)$ and $\Gamma_1(h)$, $h \in \left(0, \frac{1}{2}\right)$. The orbit $\Gamma_1\left(\frac{1}{2}\right)$, defined by $H(r_1, v) = \frac{1}{2}$ within $\rho_1 = 0$, is a separatrix, separating bounded (periodic) orbits from the unbounded ones ($H(r_1, v) \geqslant \frac{1}{2}$), see lemma 2.4 and figure 2.

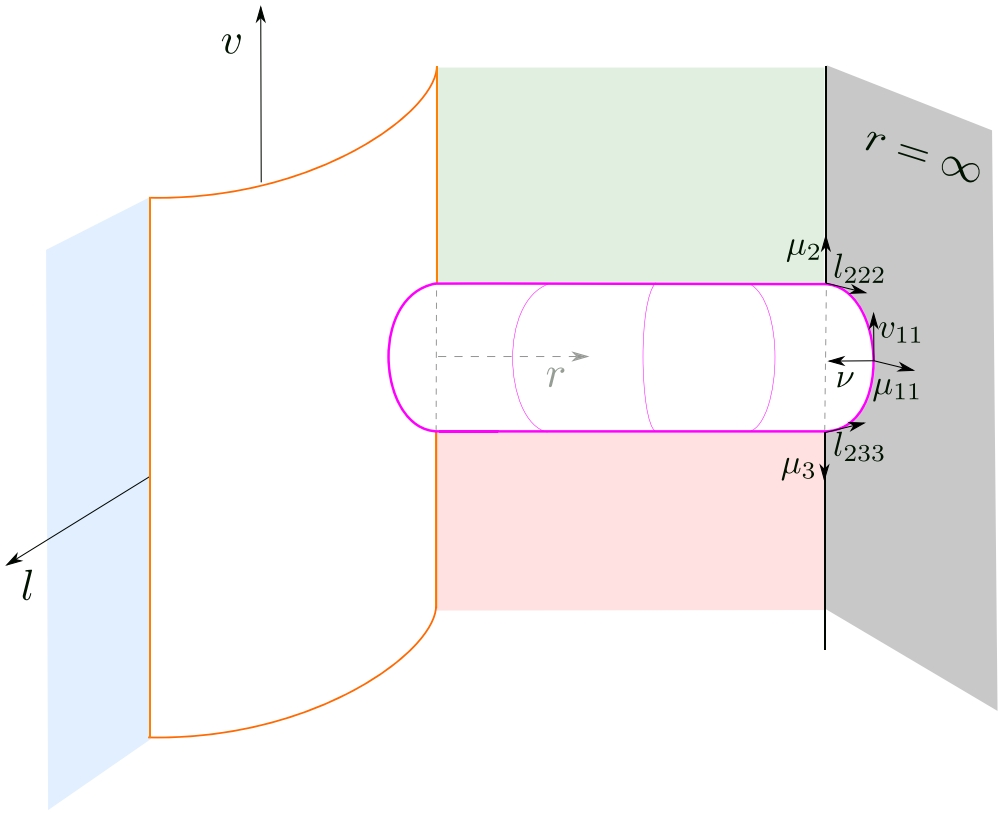

Figure 6. Illustration of the full blown up and compactified system. We indicate the coordinates used at $r=\infty$, see also (5.13)–(5.15).

5.2. *Chart* $(\bar{r}=1)_2$

By inserting (5.5) into (5.2), we obtain the equations:

$$\begin{aligned}\rho_2' &= \frac{1}{2}\rho_2 v,\\ v' &= l_2^2\left(l_2^2-1\right)-2\delta\rho_2^3 v l_2,\\ l_2' &= -\frac{1}{2}l_2\left(v+2\delta\rho_2^3 l_2\right),\end{aligned} \tag{5.17}$$

after desingularization (corresponding to division of the right hand side by ρ_2^4). Here we have two invariant planes defined by $\rho_2=0$ and $l_2=0$. Within the former, we rediscover the center at $(v,l_2)=(0,1)$ and the periodic orbits $\Gamma_2(h)$, $h\in\left(0,\frac{1}{2}\right)$, given by

$$H_2(l_2,v) := H\left(l_2^{-2},v\right)=\frac{1}{2}v^2+\frac{1}{2}-l_2^2+\frac{1}{2}l_2^4=h, \tag{5.18}$$

surrounding the center. However, $\Gamma_1\left(\frac{1}{2}\right)$ now becomes a bounded orbit $\Gamma_2\left(\frac{1}{2}\right)$, which is homoclinic to the degenerate point γ_2 defined by $(\rho_2,v,l_2)=(0,0,0)$, see figure 7. All other points $(0,v,0)$ on the v-axis, are partially hyperbolic, the linearization having eigenvalues $\pm\frac{1}{2}$, 0. All

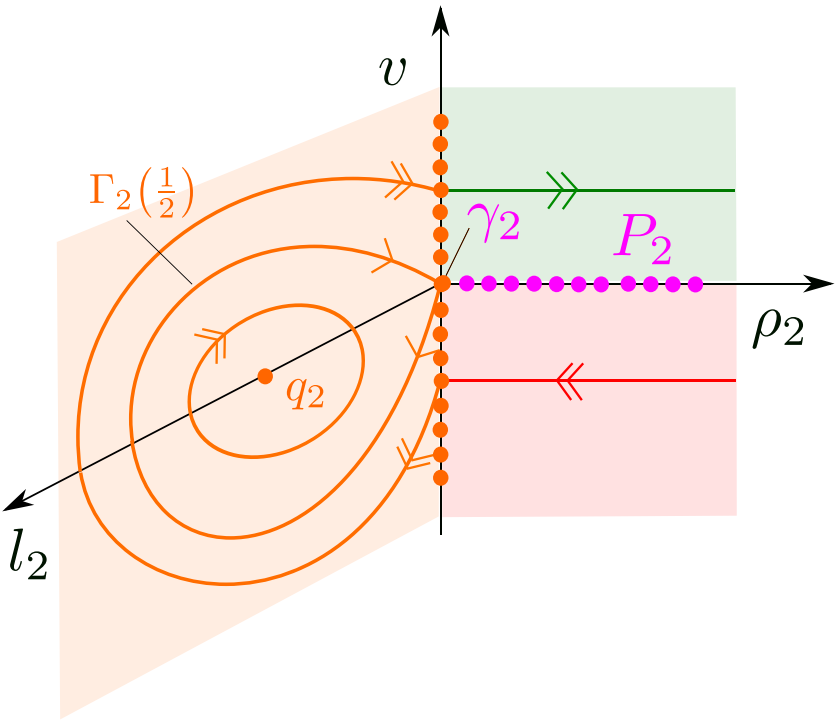

Figure 7. Dynamics in the $(\bar{r}=1)_2$-chart. Here the special orbit $\Gamma_1\left(\frac{1}{2}\right)$ in the $(\bar{l}=1)_1$-chart, becomes a homoclinic orbit $\Gamma_2\left(\frac{1}{2}\right)$ to a degenerate equilibrium γ_2.

orbits $H_2(l_2,v)=h$ with $h>\frac{1}{2}$ are heteroclinic connections within $\rho_2=0$ between points on the v-axis. Next, within $l_2=0$ we have

$$\begin{aligned}\rho_2' &= \frac{1}{2}\rho_2 v,\\ v' &= 0.\end{aligned}$$

The ρ_2-axis is the set of degenerate equilibria P_2, which is blown up by (5.6). Notice that $H_2(0,0)=\frac{1}{2}$, and since H_2 is independent of ρ_2, we conclude using (2.10) that

Lemma 5.5. $|\mathcal{E}_\infty|=1$ *on* P_2.

5.3. *Chart* $(\bar{r}=1,\bar{l}=1)_{21}$

By inserting (5.7) into (5.17), we obtain the following equations

$$\begin{aligned}\rho_2' &= \frac{1}{2}\rho_2 v_1,\\ v_1' &= \mu_1^2+\frac{1}{2}v_1^2-1-\delta\rho_2^3 v_1,\\ \mu_1' &= -\left(\frac{1}{2}v_1+\delta\rho_2^3\right)\mu_1,\end{aligned} \tag{5.19}$$

after desingularization (corresponding to division of the right hand side by μ_1). Here $\mu_1 = 0$ corresponds to the blowup of P_2, and within this invariant subspace, we have that

$$\begin{aligned} \rho_2' &= \frac{1}{2}\rho_2 v_1, \\ v_1' &= \frac{1}{2}v_1^2 - 1 - \delta\rho_2^3 v_1. \end{aligned} \tag{5.20}$$

We have two hyperbolic equilibria $\gamma_{21}^{\pm}$ along $\rho_2 = 0$ given by $v_1 = \pm\sqrt{2}$, the former is an unstable node while the latter is a stable node. As equilibria points $(0, \pm\sqrt{2}, 0)$ of the full system, they are hyperbolic saddles and the separatrix $\Gamma_1\left(\frac{1}{2}\right)$ from $(\bar{r} = 1)_1$, now denoted by $\Gamma_{21}\left(\frac{1}{2}\right)$ and given by $H_2(\mu_1, \mu_1 v_1) = \frac{1}{2}$ within $\rho_2 = 0$, is now a heteroclinic orbit connecting the two hyperbolic saddles. We summarize the findings in figure 8.

Remark 5.6. Following remark 5.3, (5.20) is equivalent to (2.3) with $l = 0$:

$$\ddot{r} = -\delta\dot{r} - \frac{1}{r^2}.$$

In particular, setting $v_1 = \rho_2 u$ with $u = \dot{r}$ and $\rho_2 = \sqrt{r}$ transforms (5.20) into

$$\begin{aligned} r' &= ur^2, \\ u' &= -\delta u r^2 - 1, \end{aligned}$$

which is studied in [36, proposition 3.1]. The advantage of working with (5.20) is that the u-axis becomes compactified. In particular, the heteroclinic orbits, connecting $\gamma_{21}^{\pm}$ within $\mu_1 = 0$, see figure 8, (called ejection-collision orbits in [35]) become unbounded in the $(r, u = \dot{r})$-coordinates.

5.4. Chart $(\bar{r} = 1, \bar{l} = 1)_{22}$

By inserting (5.8) into (5.17), we obtain the following equations

$$\begin{aligned} \rho_2' &= \frac{1}{2}\rho_2, \\ \mu_2' &= l_{22}\mu_2\left(l_{22}^3\mu_2^2 - 2\delta\rho_2^3 - l_{22}\right), \\ l_{22}' &= -l_{22}\left(l_{22}^4\mu_2^2 - \delta l_{22}\rho_2^3 - l_{22}^2 + \frac{1}{2}\right), \end{aligned} \tag{5.21}$$

after desingularization (corresponding to division of the right hand side by μ_2). All of the three invariant planes defined by $\mu_2 = 0$, $\rho_2 = 0$ and $l_{22} = 0$, respectively, are invariant. Within $\mu_2 = 0$, we find

$$\begin{aligned} \rho_2' &= \frac{1}{2}\rho_2, \\ l_{22}' &= -l_{22}\left(-\delta l_{22}\rho_2^3 - l_{22}^2 + \frac{1}{2}\right). \end{aligned} \tag{5.22}$$

Here we rediscover γ_{21}^{+} from the $(\bar{r} = 1, \bar{l} = 1)_{21}$-chart as a hyperbolic unstable node within $\mu_2 = 0$ given by

$$\gamma_{22}^{+}: \quad (\rho_2, \mu_2, l_{22}) = \left(0, 0, 1/\sqrt{2}\right),$$

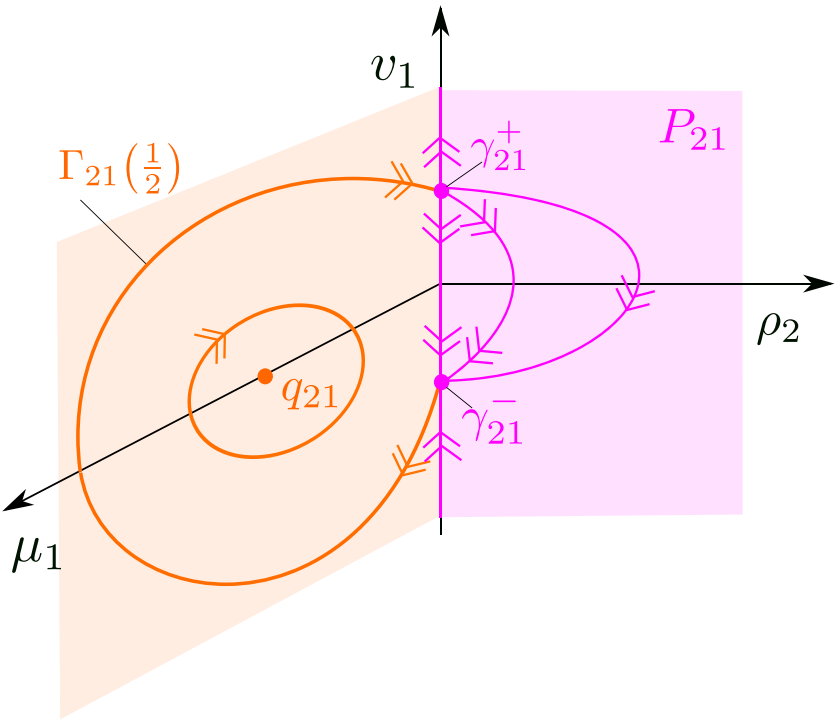

Figure 8. Dynamics in the $(\bar{r}=1,\bar{l}=1)_{21}$-chart. Here the special orbit $\Gamma_1\left(\frac{1}{2}\right)$ in the $(\bar{l}=1)_1$-chart, becomes a heteroclinic orbit $\Gamma_{21}\left(\frac{1}{2}\right)$, connecting two hyperbolic saddles $\gamma_{21}^{\pm}$.

see also (5.10). At the same time, $(\rho_2, l_{22}) = (0,0)$ is a hyperbolic saddle for (5.22), the linearization having eigenvalues $\pm\frac{1}{2}$. The two axes, ρ_2 and l_{22}, are the associated unstable and stable manifolds, respectively.

Next, within $l_{22}=0$, we have

$$\begin{aligned}\rho_2' &= \frac{1}{2}\rho_2,\\ \mu_2' &= 0,\end{aligned}$$

and the μ_2-axis is therefore a line of saddle points of (5.21), having $l_{22}=0$ ($\rho_2=0$) as its unstable manifold (stable manifold, respectively). We summarize the findings in figure 9.

5.5. *Chart* $(\bar{r}=1,\bar{l}=1)_{23}$

By inserting (5.9) into (5.17), we obtain the following equations

$$\begin{aligned}\rho_2' &= \frac{1}{2}\rho_2,\\ \mu_3' &= l_{23}\mu_3\left(l_{23}^3\mu_3^2 - 2\delta\rho_2^3 - l_{23}\right),\\ l_{23}' &= -l_{23}\left(l_{23}^4\mu_3^2 - \delta l_{23}\rho_2^3 - l_{23}^2 + \frac{1}{2}\right),\end{aligned} \tag{5.23}$$

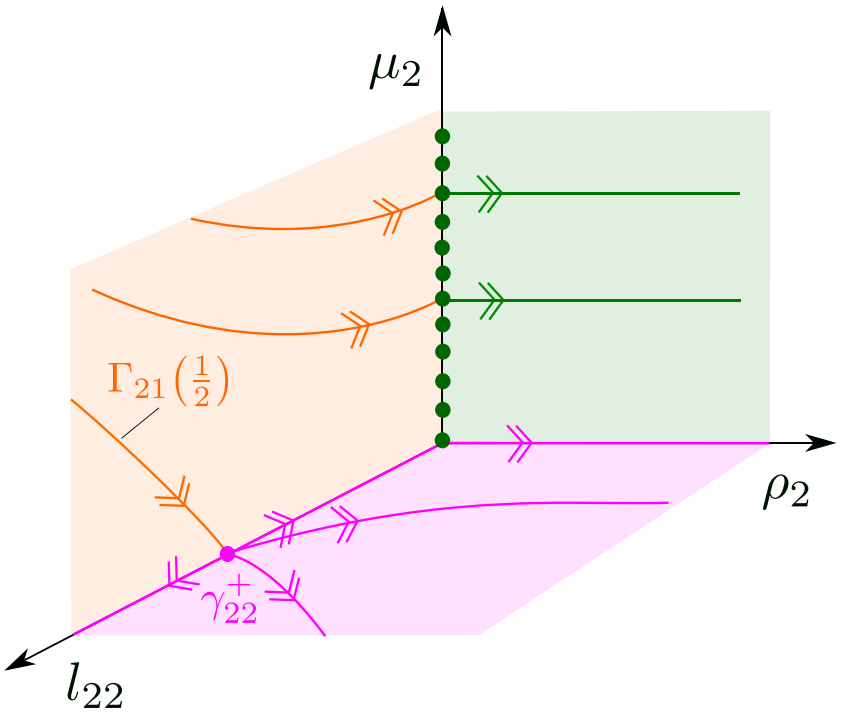

Figure 9. Dynamics in the $(\bar{r}=1,\bar{l}=1)_{22}$-chart, compare with figure 8.

after desingularization (corresponding to division of the right hand side by μ_3). The analysis in this chart is almost identical to the analysis in $(\bar{r}=1,\bar{l}=1)_{22}$. In particular, we rediscover the equilibrium point γ_{21}^{-} from the $(\bar{r}=1,\bar{l}=1)_{21}$-chart, now given by

$$\gamma_{23}^{-}: \quad (\rho_2,\mu_3,l_{23}) = \left(0,0,1/\sqrt{2}\right).$$

At the same time, we have that the μ_3-axis is line of saddle points of (5.23), having $l_{22}=0$ ($\rho_2=0$) as its stable manifold (unstable manifold, respectively). An illustration of the dynamics in this chart can be obtained by taking the time-reversal of the diagram figure 9 (replacing (a) l_{22}, μ_2 by l_{23} and μ_3, respectively, (b) γ_{22}^{+} by γ_{23}^{-} and finally (c) replacing (in line with figure 6) the color green of the invariant plane $l_{22}=0$ to red).

5.6. *Compactification in the* $(\bar{r}=1,\bar{l}=1)_{21}$*-chart*

Upon applying the transformation of (ρ_2,v_1) defined by (5.14) to the system (5.19), we obtain the following equations

$$\begin{aligned}\dot{\nu} &= -\frac{1}{2}\nu v_{11},\\ \dot{v}_{11} &= -v_{11}\left(\delta+v_{11}\right)+\nu^6\left(\mu_{11}^2\nu^6-1\right),\\ \dot{\mu}_{11} &= \mu_{11}\left(v_{11}-\delta\right),\end{aligned} \tag{5.24}$$

after desingularization (corresponding to multiplication of the right hand side by ν^3). Here $\nu=0$, which corresponds to $r=\infty$, is an invariant set, upon which we find the following:

$$\begin{aligned}\dot{v}_{11}&=-v_{11}\left(\delta+v_{11}\right),\\ \dot{\mu}_{11}&=\mu_{11}\left(v_{11}-\delta\right).\end{aligned}\tag{5.25}$$

We find two equilibria: $p_{21}^{+}:(\nu,v_{11},\mu_{12})=(0,0,0)$ and $p_{21}^{-}:(\nu,v_{11},\mu_{12})=(0,-\delta,0)$ of (5.24), both of which are hyperbolic for the reduced system (5.25) within $\nu=0$. Indeed, the linearization of (5.25) around p_{21}^{+} produces the eigenvalues $-\delta,-\delta$ (semi-simple), whereas the linearization of (5.25) around p_{21}^{-} produces $\delta,-2\delta$ as eigenvalues. Consequently, p_{21}^{+} is a stable node for (5.25), whereas p_{21}^{-} is a saddle.

The equation $\mu_{11}=0$ also defines an invariant set for (5.24), upon which we find the following:

$$\begin{aligned}\dot{\nu}&=-\frac{1}{2}\nu v_{11},\\ \dot{v}_{11}&=-v_{11}\left(\delta+v_{11}\right)-\nu^6.\end{aligned}\tag{5.26}$$

While p_{21}^{-} is clearly an unstable node for these equations, p_{21}^{+} is only semi-hyperbolic, the linearization having eigenvalues 0 and $-\delta$. It is a simple calculation, to show that the associated center manifold $W^c(p_{21}^{+})$ takes the following graph form:

$$W^c\left(p_{21}^{+}\right):\quad v_{11}=-\frac{1}{\delta}\nu^6\left(1+\mathcal{O}\left(\nu^6\right)\right).\tag{5.27}$$

The $\mathcal{O}(\nu^6)$-term is a smooth function of ν^6 (and δ). This follows from the fact that the first equation of (5.26) can be written as $(\nu^6)'=-3\nu^6 v_{11}$. Inserting (5.27) into (5.26) gives

$$\dot{\nu}=\frac{1}{2\delta}\nu^7\left(1+\mathcal{O}\left(\nu^6\right)\right),$$

and $\nu>0$ is therefore increasing on $W^c(p_{21}^{+})$. The center manifold is therefore unique as the unstable set of p_{21}^{+} and p_{21}^{+} is a nonhyperbolic saddle for (5.26). We illustrate our findings in figure 10.

Remark 5.7. It is a simple calculation to show that the time used in (5.24) coincides with the original time in (5.1), which is why we use $\dot{()}$ instead of $()'$, recall remark 2.1.

Using (5.5), (5.12) and (5.14), we can write (5.27) in the $(r,\dot{r})$-plane as a graph

$$\dot{r}=-\frac{1}{\delta r^2}\left(1+\mathcal{O}\left(r^{-3}\right)\right),$$

over $r\gg 1$. We see that $\dot{r}\to 0$ on W^c as $t\to-\infty$, in line with the results of [35, proposition 3.1].

5.7. Compactification in the $(\bar{r}=1,\bar{l}=1)_{22}$-chart

Upon applying the transformation of (ρ_2,l_{22}) defined by (5.13) to the system (5.21), we obtain the following equations

$$\begin{aligned}\nu'&=-\frac{1}{2}\nu,\\ \mu_2'&=-\mu_2 l_{222}\left(2\delta+\nu^6 l_{222}-\nu^{12}l_{222}^3\mu_2^2\right),\\ l_{222}'&=l_{222}\left(1+\delta l_{222}+\nu^6 l_{222}^2-\nu^{12}l_{222}^4\mu_2^2\right).\end{aligned}\tag{5.28}$$

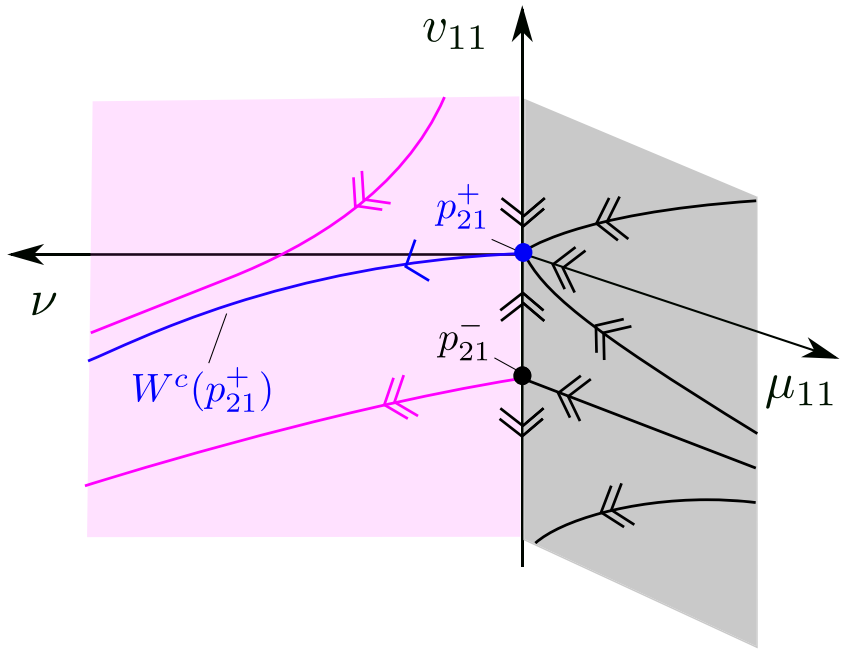

Figure 10. Dynamics of (5.24). The point p_{21}^- is fully hyperbolic, whereas p_{21}^+ is only semi-hyperbolic (we use single-headed arrows to separate center directions from hyperbolic directions (double-headed arrows)). The center manifold $W^c(p_{21}^+)$ of p_{21}^+ is unique as the unstable set of p_{21}^+.

Here $l_{222}=0$ defines an invariant set upon which we have $\nu'=-\frac{1}{2}\nu$ and $\mu_2'=0$. Since $l_{222}=0$ corresponds to $l_{22}=0$, see (5.13), these findings are obviously in agreement with the results in the $(\bar{r}=1,\bar{l}=1)_{22}$-chart whenever $\nu>0$, see section 5.4 and figure 9 (green plane). On the other hand, $\nu=0$, corresponding to $r=\infty$, is now an invariant set of (5.28). In fact, $\nu=l_{222}=0$ is a line of saddle points; the linearization of (5.28) about any point in this set having eigenvalues $-\frac{1}{2},0,1$. The stable manifold of $\nu=l_{222}=0$ is the (ν,μ_2)-plane, whereas the associated unstable set is the (μ_2,l_{222})-plane. Setting $\nu=0$ in (5.28) gives

$$\begin{aligned}\mu_2' &= -2\delta\mu_2 l_{222},\\ l_{222}' &= l_{222}\left(1+\delta l_{222}\right),\end{aligned}$$

which has no equilibria within the first quadrant. In particular, $l_{222}>0$ (μ_2) is monotonically increasing (decreasing, respectively). Finally, within $\mu_2=0$ we have

$$\begin{aligned}\nu' &= -\frac{1}{2}\nu,\\ l_{222}' &= l_{222}\left(1+\delta l_{222}+\nu^6 l_{222}^2\right),\end{aligned}$$

having a hyperbolic saddle at the origin. We summarize the local findings in figure 11.

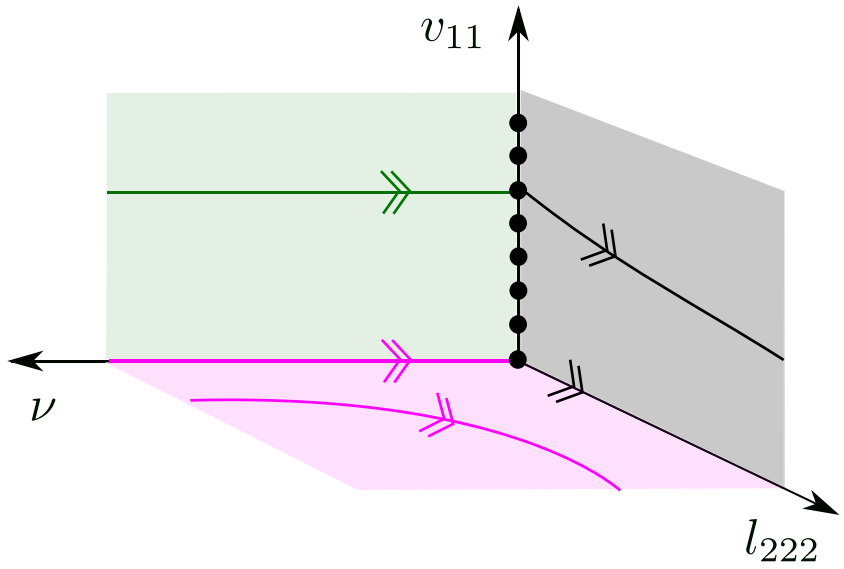

Figure 11. Dynamics of (5.28). The v_{11}-axis is a line of saddle-points. There are no other equilibria in this chart.

5.8. *Compactification in the* $(\bar{r}=1,\bar{l}=1)_{23}$*-chart*

Upon applying the transformation of (ρ_2, l_{22}) defined by (5.13) to the system (5.21), we obtain the following equations

$$\begin{aligned}\nu' &= \frac{1}{2}\nu,\\ \mu_3' &= \mu_3 l_{233}\left(2\delta - \nu^6 l_{233} - \nu^{12} l_{233}^3 \mu_3^2\right),\\ l_{233}' &= l_{233}\left(-1 + \delta l_{233} - \nu^6 l_{233}^2 + \nu^{12} l_{233}^4 \mu_3^2\right).\end{aligned} \tag{5.29}$$

The analysis of these equations is almost identical to the analysis performed in sections 5.6 and 5.7. We therefore only present a diagram, see figure 12.

Upon combining all of our findings in the local charts, we obtain the global perspective in figure 1 (using the geometric viewpoint in figure 6). Notice that from this perspective it follows directly that any $\Gamma(h)$ with $h > \frac{1}{2}$ cannot be the ω-limit set. We elaborate further upon this in the following section.

6. Discussion

In this paper, we have revisited the linearly damped Kepler problem (1.1) with the main purpose of describing smoothness properties of the invariant manifolds obtained in [36], see theorems 2.7 and 2.8. In the process, we identified a separate invariant manifold $W^s(q)$, see theorem 2.6. This one-dimensional manifold of (2.3), corresponding to orbits becoming more circular as $t \to \infty$, acts as the center of oscillations along the invariant manifolds of theorems 2.7 and 2.8, see figure 1. Finally, in section 5 we performed a blowup analysis that led to the geometric description of the dynamics illustrated in figure 1.

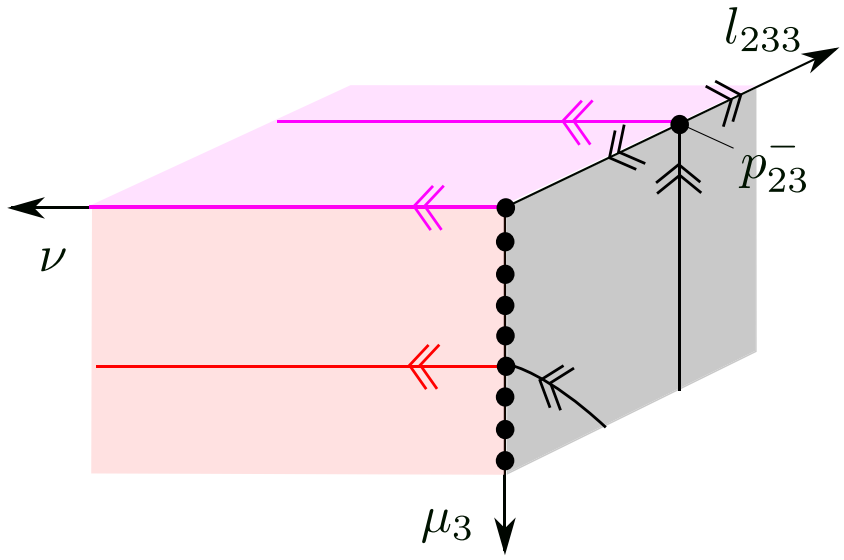

Figure 12. Dynamics of (5.29). The hyperbolic point p_{23}^- corresponds to the point p_{22}^-, see figure 10, upon the coordinate transformation defined by $l_{233} = -\nu_{11}^{-1}$. The μ_3-axis is a line of saddle-points.

Poincaré [40] considered (1.1) with the following general $(u,\dot{u})$-dependent δ:

$$\delta(u,\dot{u}) = \frac{k|\dot{u}|^\alpha}{|u|^\beta}, \tag{6.1}$$

for $\beta,\alpha \geqslant 0$ and $k>0$, see also [33]. He argued formally, that for all α and β sufficiently large, orbits tend to 'circularize', in the sense that $\mathcal{E}(u(t),\dot{u}(t)) \to 0$ for $t \to t_{\max}$ on an open set of initial conditions $(u(0),\dot{u}(0)) \in (\mathbb{R}^2 \setminus \{0\}) \times \mathbb{R}^2$. Here $t_{\max} > 0$ is time of collision: $u(t) \to 0$ for $t \to t_{\max}^-$. In the recent preprint [28], we used the approach of the present paper (based upon blowup and normal form theory) to address this issue of circularization from a rigorous point of view. Interestingly, in contrast to the claim of Poincaré, we find that circularization only occurs for $\alpha + 2\beta < 3$ and moreover that it implies finite time blowup of solutions (i.e. $t_{\max} < \infty$). We emphasize that it is known that circularization does not occur for linear damping (indeed, it is exceptional according to theorems 2.6 and 2.7, occurring only a zero measure set) nor does it occur for the Poynting-Plummer-Damby damping ($\alpha = 0$, $\beta = 2$). See [9, 33] for a general analysis of the case $\alpha = 0$, $\beta > 0$. In future work, we will use the same approach—in combination with compactification, as in section 5—to address existence of unbounded dynamics within the general class of damping functions (6.1).

In the following, we will use the geometric framework of the blowup approach to shed light on $|\mathcal{E}_\infty| \to 1$, recall lemma 5.1.

Firstly, in figure 13 we have used Matlab's ODE15s to simulate the system for initial conditions near the set $\Gamma_2(0.8)$ defined by $\rho_2 = 0$, $H_2(l_2,\nu) = 0.8 > \frac{1}{2}$, recall (5.18). More specifically, in (a) we use the coordinates (ρ_2,ν,l_2) of the $(\bar{r}=1)_2$-chart, see (5.5), and select 50 initial conditions (indicated by the cyan cylinder near $\nu = 0$) with $(l_2,\nu,\rho_2) = (l_{20},0,\rho_{20})$, $H_2(l_{20},0) = 0.8 > \frac{1}{2}$, and ρ_{20} in the interval $(0.15,0.25)$ (equispaced). The curve $\Gamma_2(0.8)$ is shown in red and the forward orbits (also in cyan) follow this red curve, but only up until a

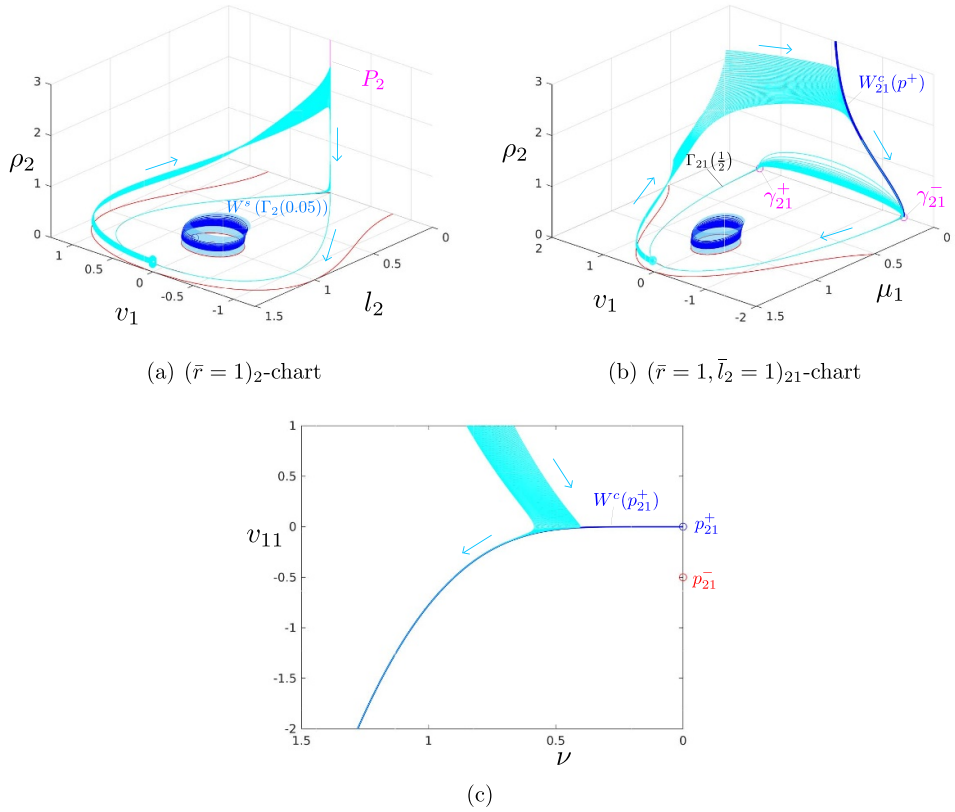

(a) $(\bar{r}=1)_2$-chart (b) $(\bar{r}=1,\bar{l}_2=1)_{21}$-chart

(c)

Figure 13. Numerical forward integration (using Matlab's ODE15s with low tolerances) of initial conditions (cyan cylinder near $v=0$) starting close to a $h=0.8$ level set of the Hamiltonian function H_2 within $\rho_2=0$ (red curves in (a) and (b)). The corresponding orbits (also in cyan) follow an itinerary that can be explained by our blowup analysis (see text and compare with figure 14 below). In (a) we use the (ρ_2,v,l_2)-coordinates of the $(\bar{r}=1)_2$-chart, whereas in (b) we use the (ρ_2,v_1,μ_1)-coordinates of the $(\bar{r}=1,\bar{l}_2=1)_{21}$-chart. In (c) we use a projection onto the (ν,v_{11})-plane, see (5.14). Here we see that the cyan orbits all follow the center manifold $W^c(p^+_{21})$ which lead these orbits towards γ^-_{21} and $\Gamma_{21}\left(\frac{1}{2}\right)$, see (b).

vicinity of the v-axis (due to the saddle-structure along this set, see figure 7 and the discussion of figure 14 below). From here ρ_2 increases and the orbits eventually contract towards the degenerate set P_2. In (b), we use the coordinates (ρ_2,v_1,μ_1) of the $(\bar{r}=1,\bar{l}_2=1)_{21}$-chart, where P_2 has been blown up, to illustrate the same (computed) orbits. Here we see that the motion along P_2 in (a) is due to the contraction towards the center manifold $W^c(p^+_{21})$; this is also shown in (c) using a projection onto the (ν,v_{11})-plane, recall (5.14). Beyond the motion along $W^c(p^+)$ in figure 13(b), the cyan curves come close together near γ^-_{21} and follow the heteroclinic orbit $\Gamma_{21}\left(\frac{1}{2}\right)$, connecting γ^-_{21} and γ^+_{21}. Once passing close to γ^+_{21} the cyan curves move close to the $\mu_1=0$ plane again before returning to γ^-_{21} and $\Gamma_{21}\left(\frac{1}{2}\right)$. This process repeats itself. The computations were performed with low tolerances (10^{-12}) and ended when the value of l reached a value of 10^{-4}.

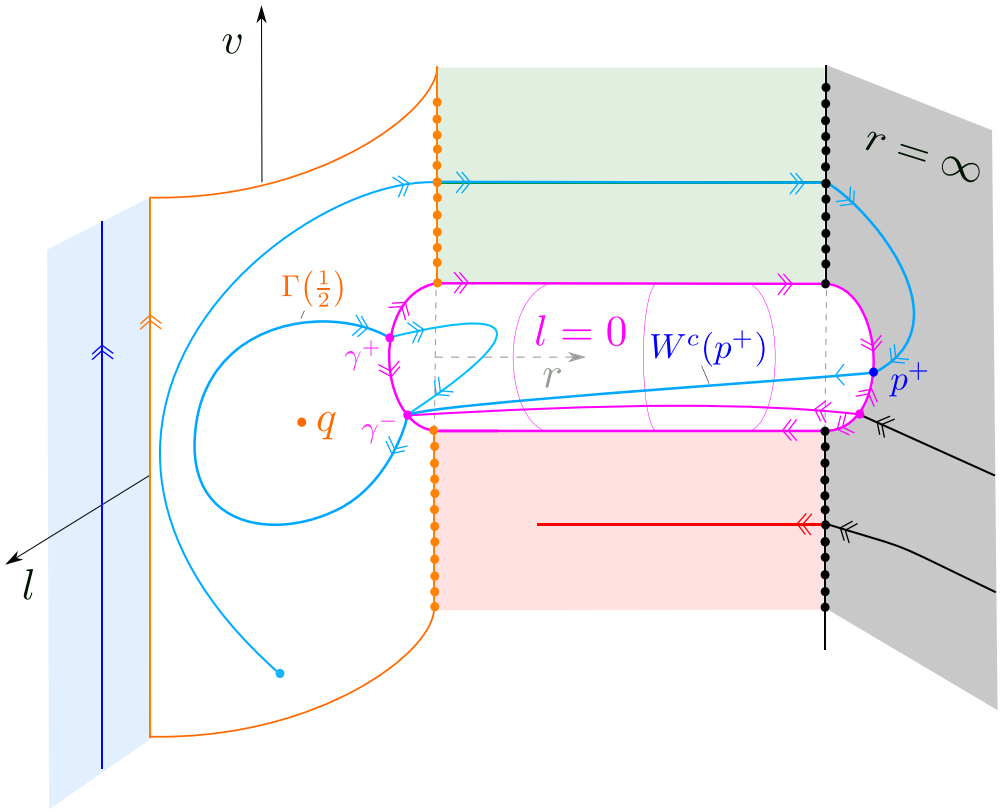

Figure 14. The forward flow of an initial condition (cyan disc) with sufficiently small angular momentum $0<l\ll 1$ and near a $h>\frac{1}{2}$ level set of the Hamiltonian function H, will follow the 'singular orbit' in cyan (i.e. the forward orbit will remain $o(1)$-close to local copies of this cyan curve in the local charts as the initial value of the angular momentum $l\to 0^+$), at least up until γ^+, see figure 13.

The results in figure 13 are in agreement with the findings in section 5 (see figure 1). We emphasize this point further in figure 14, where we illustrate a 'singular' orbit of a point on the orange cylinder. Here singular refers to the fact that it lies on the blowup space (it is therefore not a true orbit of the system (1.1) since it occurs on $r=0$) and at the same time we use a concatenation of unstable and stable manifolds across saddle points. The forward orbit of initial conditions starting near the cyan curve on the orange cylinder (with $0<l\ll 1$) (as in figure 13 in the local charts $(\bar{r}=1)_2$ and $(\bar{r}=1,\bar{l}_2=1)_{21}$) will track this curve (meaning that the orbit remains close to local copies within compact subsets of the local charts) up until γ^+. This follows from section 5, but we will leave out further details.

At γ^+ there is no unique forward (singular) orbit, since γ^+ is an unstable node on $\mu=0$ (the $l=0$ cylinder corresponding to the blowup of P_2, see (5.6)), see also figure 8. Nevertheless, since (a) γ^+ connects to γ_-, (b) γ_- is contracting on $\rho=0$, and (c) $\Gamma\left(\frac{1}{2}\right)$ connects back to γ^+ this process repeats itself for an actual orbit, starting near the cyan disc with $0<l\ll 1$. However, since l is monotonically decreasing, the excursions from γ^+ to γ^- will get closer and closer to the purple connection (along the half-circle $(\bar{v},\bar{l}_2)\in S^1$ $\bar{l}_2\geqslant 0$ within $\rho_2=0$). We observe this numerically (also indicated in figure 13(b) by the blue segments close to $\mu_1=0$).

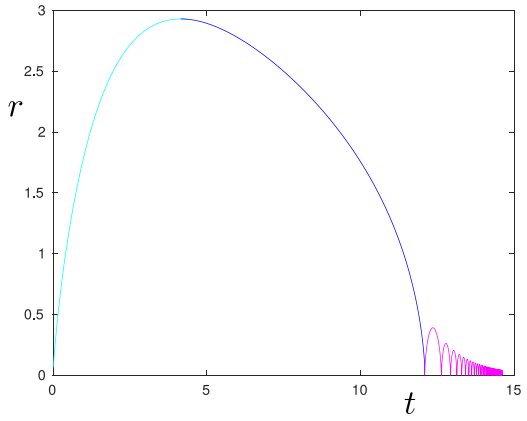

Figure 15. $r(t)$ along one of the cyan curves in figure 13. The curve has been divided into three parts: cyan, blue and purple and these are characterized as follows. The first cyan part corresponds to an increase in r due to the line of saddle points along the v-axis in figure 13(a). This is followed by the blue part, which corresponds to a capture-collision type motion (in phase space this part occurs due to the attraction towards the center manifold $W^c(p_{21}^+)$). The final part in purple, corresponds to repeated ejection-collision type oscillations, the amplitude of which are decreasing.

However, and this is the main point, since $\Gamma_1\left(\frac{1}{2}\right)$ cannot be the ω-limit set, see lemma 5.1, and since $l=0$ is invariant, the ω-limit set of the initial conditions in figure 13 (or near the cyan disc in figure 14) has to be $\Gamma_1(h)$ with $h<\frac{1}{2}$ but $h\sim\frac{1}{2}$. In other words, these initial conditions belong to a $W^s(\Gamma(h))$ for some $h\in(0,\frac{1}{2})$, where $h\to\frac{1}{2}$ as $l_0\to 0$. The implication of this is that the cylinders $W^s(\Gamma(h))$ have a dramatic limit $h\to\frac{1}{2}$ (corresponding to $|\mathcal{E}_\infty|\to 1^-$ see (2.10)). Indeed, the two-dimensional cylindrical manifolds $W^s(\Gamma(h))$ with $h<\frac{1}{2}$ but $h\sim\frac{1}{2}$ open up like a flower, stretching (and collapsing for $h\to\frac{1}{2}$) both along the orange and the purple cylinder in figure 14 (corresponding to r very small and very large, respectively).

At the same time, $l=0$ defines an invariant set (of collinear orbits) and the ω-limit set of any point within this set is γ^-. Orbits having γ^+ as the α-limit set (within $l=0$) are called ejection-collision orbits, whereas orbits having either p^- or p^+ as the α-limit set (going along $W^s(p_{21}^+)$ in the latter case) are referred to as capture-collision orbits, see e.g. [9, 35]. Interestingly, the orbits in figure 13 with $0<l\ll 1$ exhibit both types of behaviour, first capture-collision by following close to $W^c(p_{21}^+)$ and then subsequently (and repeatedly) ejection-collision type behaviour by passing close to γ^+ and γ^-. We illustrate this in our final figure 15 plotting r as a function of t along one of the cyan curves in figure 13(a).

Data availability statement

No new data were created or analysed in this study.

Acknowledgments

The author wishes to thank Sam Jelbart and Rafael Ortega for providing valuable feedback on earlier versions of the manuscript. In particular, the author is grateful for the references

provided by Sam Jelbart on the regularization of binary collisions and for Rafael Ortega's helpful comments on the energy-angle coordinates.

Appendix. Proof of lemma 4.10

We consider (4.17), repeated here for convenience

$$\begin{aligned}\frac{dH}{d\tau} &= \frac{1}{3\delta}x\left(\Lambda\left(H,x\right)+x^N R\left(H,\phi,x\right)\right),\\ \frac{d\phi}{d\tau} &= \frac{1}{3\delta x^2}\left(\Omega\left(H,x\right)+x^{N+1}P\left(H,\phi,x\right)\right),\\ \frac{dx}{d\tau} &= -1,\end{aligned} \tag{A.1}$$

for $x>0$. We then apply $\frac{\partial^{|\nu|}}{\partial\tau^{\nu_1}\partial H_0^{\nu_2}\partial\phi_0^{\nu_3}\partial x_0^{\partial\nu_4}}$ on both sides of these equations; recall the notation defined in (4.24). We then obtain $\frac{d}{d\tau}\underline{H}_\nu$, $\frac{d}{d\tau}\underline{\phi}_\nu$ and $\frac{d}{d\tau}\underline{x}_\nu$ on the left hand sides, respectively. Obviously,

$$x_\nu \equiv 0 \text{ unless } \nu=(1,0,0,0)\,,\ \text{or } \nu=(0,0,0,1)\,, \tag{A.2}$$

where $x_{(1,0,0,0)}=-1, x_{(0,0,0,1)}=1$.

To handle the associated right hand sides of (A.1) that occur after application of $\frac{\partial^{|\nu|}}{\partial\tau^{\nu_1}\partial H_0^{\nu_2}\partial\phi_0^{\nu_3}\partial x_0^{\partial\nu_4}}$, we use the Faa di Bruno formula [7]: For $\nu=(\nu_1,\ldots,\nu_d)\in\mathbb{N}_0$, $z=(z_1,\ldots,z_d)$, $d\in\mathbb{N}$, define

$$\begin{aligned}\nu! &:= \prod_{i=1}^d \nu_i!,\\ D^\nu &:= \frac{\partial^{|\nu|}}{\partial z_1^{\nu_1}\cdots\partial z_d^{\nu_d}},\\ [z]^\nu &:= \prod_{i=1}^d z_i^{\nu_i}.\end{aligned}$$

Moreover, if we also consider $\mu=(\mu_1,\ldots,\nu_d)$, then we write $\mu\prec\nu$ provided at least one of the conditions hold:

(1) $|\mu|<|\nu|$;
(2) $|\mu|=|\nu|$ and $\mu_1<\nu_1$; or
(3) $|\mu|=|\nu|$, $\mu_1=\nu_1,\ldots,\mu_k=\nu_k$ and $\mu_{k+1}<\nu_{k+1}$ for some $1\leqslant k<d$.

Finally, we write $0=(0,\ldots,0)$ in $\mathbb{N}_0^d$.

Lemma A.1. [7, *theorem 2.1*] *Consider smooth functions* $F:\mathbb{R}^m\to\mathbb{R}$ *and* $G=(G_1,\ldots,G_m):\mathbb{R}^d\to\mathbb{R}^m$, *and define*

$$W(z) := (F\circ G)(z)\,.$$

Then

$$D^{\nu}W=\sum_{1\leqslant|\lambda|\leqslant n}D^{\lambda}F\sum_{s=1}^{n}\sum_{p_s(\nu,\lambda)}(\nu!)\prod_{j=1}^{s}\frac{\left[D^{l_j}G_1,\ldots,D^{l_j}G_m\right]^{k_j}}{(k_j!)\,(l_j)^{|k_j|}}, \tag{A.3}$$

where $n=|\nu|$ *and*

$$\begin{aligned}p_s(\nu,\lambda):=\Big\{&(k_1,\ldots,k_s,l_1,\ldots,l_s):|k_i|>0,\\&0\prec l_1\prec\cdots\prec l_s,\\&\sum_{i=1}^{s}k_i=\lambda,\quad\sum_{i=1}^{s}|k_i|l_i=\nu\Big\}.\end{aligned} \tag{A.4}$$

We now consider the following functions:

$$\begin{aligned}W_R&=\underline{x}^{N+1}.R\circ\left(\underline{H},\underline{\phi},\underline{x}\right),\\W_P&=\underline{x}^{N-1}.P\circ\left(\underline{H},\underline{\phi},\underline{x}\right),\end{aligned}$$

of $(\tau,H_0,\phi_0,x_0)\in V(\xi)$, which appear on the right hand side of (A.1). Here $V(\xi)$ is defined in (4.18), repeated here for convenience:

$$V(\xi):=\left\{(\tau,H_0,\phi_0,x_0)\in(0,\xi)\times J\times\mathbb{T}\times(0,\xi):0<\tau<x_0\right\}.$$

Lemma A.2. *Let* $M\in\mathbb{N}$ *be so that* $N-2M\geqslant 0$*. Suppose that*

$$|\underline{H}_{\nu}(\tau,H_0,\phi_0,x_0)|\leqslant C_M,\quad|\underline{\phi}_{\nu}(\tau,H_0,\phi_0,x_0)||\tau-x_0|^{1+\nu_1+\nu_4}\leqslant C_M,$$

for all $(\tau,H_0,\phi_0,x_0)\in V(\xi)$ *and all* $1\leqslant|\nu|\leqslant M$*. Then there exists a constant* $K=K(M,|R|_{C^M},|P|_{C^M},C_M)>0$*, depending only on: (a)* M*, (b) uniform* C^M *bounds* $|R|_{C^M}$ *and* $|P|_{C^M}$ *of* R *and* P*, respectively, and (c)* $C_M>0$*, such that*

$$\begin{aligned}|D^{\nu}W_R(\tau,H_0,\phi_0,x_0)|&\leqslant K|\tau-x_0|^{N+1-\nu_1-\nu_4-|\nu|},\\|D^{\nu}W_P(\tau,H_0,\phi_0,x_0)||\tau-x_0|^2&\leqslant K|t-x_0|^{N+1-\nu_1-\nu_4-|\nu|},\end{aligned}$$

for all $(\tau,H_0,\phi_0,x_0)\in V(\xi)$ *and all* $1\leqslant|\nu|\leqslant M$*.*

Proof. We focus on W_R. The estimate of W_P can be obtained in a completely analogous way. First, we write

$$D^{\nu}W_R=D^{(\nu_1,0,0,\nu_4)}\left(\underline{x}^{N+1}.D^{(0,\nu_2,\nu_3,0)}\underline{R}\right),$$

using (A.2). Here we use $D^{\nu}\underline{R}$ to denote the partial derivatives of the composition function $R(\underline{H}(),\underline{\phi}(),\underline{x}())$. Then by the product rule, we have

$$\begin{aligned}D^{\nu}W_R=\sum_{q_4=0}^{\nu_4}\sum_{q_1=0}^{\nu_1}(-1)^{\nu_1-q_1}\binom{\nu_4}{q_4}\binom{\nu_1}{q_1}\binom{N+1}{\nu_4-q_4+\nu_1-q_1}(\nu_4-q_4+\nu_1-q_1)!\\\times\underline{x}^{N+1-\nu_4+q_4-\nu_1+q_1}D^{(q_1,\nu_2,\nu_3,q_4)}\underline{R},\end{aligned} \tag{A.5}$$

using (A.2) again. We then use lemma A.1, in particular (A.3) with $\nu = (q_1, \nu_2, \nu_3, q_4)$, $d = 4$, $m = 3$, $D^{l_j} G_1 = \underline{H}_{l_j}$, $D^{l_j} G_2 = \underline{\phi}_{l_j}$, $D^{l_j} G_3 = \underline{x}_{l_j}$, to estimate $D^{(q_1,\nu_2,\nu_3,q_4)}\underline{R}$:

$$\begin{aligned}
|D^{(q_1,\nu_2,\nu_3,q_4)}\underline{R}| &\leqslant K_0 \sum_{p_s((q_1,\nu_2,\nu_3,q_4),\lambda)} \prod_{j=1}^{s} |\underline{H}_{l_j}|^{k_{j,1}} |\underline{\phi}_{l_j}|^{k_{j,2}} |\underline{x}_{l_j}|^{k_{j,3}} \\
&\leqslant K_0 \sum_{p_s((q_1,\nu_2,\nu_3,q_4),\lambda)} \prod_{j=1}^{s} C_M^{|k_j|} |\underline{x}|^{-k_{j,2}(1+l_{j,1}+l_{j,4})} \\
&\leqslant K_0 C_M^M |\underline{x}|^{-q_1-q_4},
\end{aligned}$$

writing $k_j = (k_{j,1}, k_{j,2}, k_{j,3})$, $l_j = (l_{j,1}, \ldots, l_{j,4})$, for some $K_0 = K_0(M, |R|_{C^M}) > 0$ depending only on: (a) M and (b) the C^M bound $|R|_{C^M}$ on the smooth function R. In the final inequality, we have used the definition of p_s (A.4). Specifically, from

$$\sum_{j=1} k_{j,2}\,(1 + l_{j,1} + l_{j,2}) < \sum_{j=1} |k_j|\,(1 + l_{j,1} + l_{j,2}) \leqslant \sum_{j=1} |\nu|\,(1 + l_{j,1} + l_{j,2}) \leqslant 1 + q_1 + q_2. \tag{A.6}$$

we have concluded that $\sum_{j=1} k_{j,2}(1 + l_{j,1} + l_{j,2}) \leqslant q_1 + q_2$; notice that the first inequality in (A.6) is *strict*. Now using (A.5), we have

$$|D^\nu W_R| \leqslant K|\tau - x_0|^{N+1-\nu_1-\nu_4},$$

for $K = K(M, |R|_{C^M}, C_M) > 0$ large enough. □

Finally, we describe the the functions

$$W_\Lambda = \underline{x}.\Lambda \circ (\underline{H}, \underline{x}), \quad W_\Omega = \underline{x}^{-2}.\Omega \circ (\underline{H}, \underline{x}),$$

that also appear on the right hand side (A.1), but are independent of $\underline{\phi}$.

Lemma A.3. *Let $M \in \mathbb{N}$ and suppose that*

$$|\underline{H}_\nu(\tau, H_0, \phi_0, x_0)| \leqslant C_M,$$

for all $(\tau, H_0, \phi_0, x_0) \in V(\xi)$ and all $1 \leqslant |\nu| \leqslant M$. Then there exists a constant $K = K(M, |D|_{C^M}, |\Omega|_{C^M}, C_M) > 0$, depending only on: (a) M, (b) uniform C^M bounds $|D|_{C^M}$ and $|\Omega|_{C^M}$ of D and Ω, respectively, and (c) on a constant $C_M > 0$, such that

$$|D^\nu W_\Lambda(\tau, H_0, \phi_0, x_0)| \leqslant K, \quad |D^\nu W_\Omega(\tau, H_0, \phi_0, x_0)|\,|\tau - x_0|^{2+\nu_1+\nu_4} \leqslant K,$$

for all $(\tau, H_0, \phi_0, x_0) \in V(\xi)$ and all $1 \leqslant |\nu| \leqslant M$.

Proof. Follows from a direct calculation. □

Lemma A.4. *Let $M = \lfloor \frac{N}{2} \rfloor$. Then for any $\nu \in \mathbb{N}_0$ with $|\nu| \leqslant M$ there exists a constant C_ν and a $\xi_\nu > 0$ such that*

$$|\underline{H}_\nu(\tau, H_0, \phi_0, x_0)| \leqslant C_\nu, \quad |\underline{\phi}_\nu(\tau, H_0, \phi_0, x_0)|\,|\tau - x_0|^{1+\nu_1+\nu_4} \leqslant C_\nu, \tag{A.7}$$

for all $(\tau, H_0, \phi_0, x_0) \in V(\xi_\nu)$.

Upon proceeding as in the proof of lemma 4.6, (A.7) implies that $\underline{H}_\nu$ extends continuously to $\overline{V(\xi)}$. Consequently, we complete the proof of lemma 4.10 by proving lemma A.4.

To prove lemma A.4, we proceed by induction. It is true for $\nu = \mathbf{0}$, see (4.20) and the proof of lemma 4.5. Next, suppose that it is true for $|\nu| = n$. We then consider $\nu' := \nu + \delta_i$, with $\delta_i = (\delta_{i,1}, \ldots, \delta_{i,4})$ for

$$\delta_{i,j} = \begin{cases} 1 & j = i, \\ 0 & j \neq i. \end{cases}$$

Lemma A.5. *For $\widetilde{C}_{\nu'} > 0$ large enough and $\xi > 0$ small small enough, we have that*

$$|\underline{H}_{\nu'}(0, H_0, \phi_0, x_0)| \leqslant \widetilde{C}_{\nu'}, \quad |\underline{\phi}_{\nu'}(0, H_0, \phi_0, x_0)||x_0|^{1+\nu_1+\nu_4+\delta_{i,1}+\delta_{i,4}} \leqslant \widetilde{C}_{\nu'},$$

for all $(0, H_0, \phi_0, x_0) \in V(\xi)$

Proof. By definition $\underline{H}(0, H_0, \phi_0, x_0) = H_0$, $\underline{\phi}(0, H_0, \phi_0, x_0) = \phi_0$, $\underline{x}(0, H_0, \phi_0, x_0) = x_0$. Consequently, if $\nu = (0, \nu_2, \nu_3, \nu_4)$ then $\underline{z}_\nu(0, \ldots) = 0$ for $z = H, \phi, x$ (unless $\underline{H}_{(0,1,0,0)} = 1$, $\underline{\phi}_{(0,0,1,0)} = 1$, or $\underline{x}_{(0,0,0,1)} = 1$). On the other hand, if $\nu_1 \geqslant 1$ then by (A.1)

$$\begin{aligned}
\underline{H}_{\nu+\delta_i}\big|_{\tau=0} &= \frac{1}{3\delta}\Big(D^{(\nu_1-1,\nu_2,\nu_3,\nu_4)+\delta_i}\left(\underline{x}.\Lambda\left(\underline{H},\underline{x}\right)\right)_{\tau=0} \\
&\quad + D^{(\nu_1-1,\nu_2,\nu_3,\nu_4)+\delta_i}\left(\underline{x}^{N+1}.R\left(\underline{H},\underline{\phi},\underline{x}\right)\right)_{\tau=0}\Big), \\
\underline{\phi}_{\nu+\delta_i}\big|_{\tau=0} &= \frac{1}{3\delta}\Big(D^{(\nu_1-1,\nu_2,\nu_3,\nu_4)+\delta_i}\left(\underline{x}^{-2}.\Omega\left(\underline{H},\underline{x}\right)\right)_{\tau=0} \\
&\quad + D^{(\nu_1-1,\nu_2,\nu_3,\nu_4)+\delta_i}\left(\underline{x}^{N-1}.P\left(\underline{H},\underline{\phi},\underline{x}\right)\right)\Big)_{\tau=0}.
\end{aligned}$$

The result then follows upon using the induction hypothesis, lemmas A.2 and A.3. □

We now consider

$$\begin{aligned}
\frac{d\underline{H}_{\nu'}}{d\tau} &= \frac{1}{3\delta}\left(D^{\nu'}\left(\underline{x}.\Lambda\left(\underline{H},\underline{x}\right)\right) + D^{\nu'}\left(\underline{x}^{N+1}.R\left(\underline{H},\underline{\phi},\underline{x}\right)\right)\right), \\
\frac{d\underline{\phi}_{\nu'}}{d\tau} &= \frac{1}{3\delta}\left(D^{\nu'}\left(\underline{x}^{-2}.\Omega\left(\underline{H},\underline{x}\right)\right) + D^{\nu'}\left(\underline{x}^{N-1}.P\left(\underline{H},\underline{\phi},\underline{x}\right)\right)\right).
\end{aligned}$$

Let $C_{H,\nu'} := 2\widetilde{C}_{\nu'}$ and $C_{\phi,\nu'} > \widetilde{C}_{\nu'}$. We may take $\widetilde{C}_{\nu'}$ large enough such that $\widetilde{C}_{\nu'} \geqslant C_\nu$ for all $|\nu| \leqslant n$. Then by lemma A.5, we have that

$$|\underline{H}_{\nu'}(\tau, H_0, \phi_0, x_0)| \leqslant C_{H,\nu'}, \quad |\underline{\phi}_{\nu'}(\tau, H_0, \phi_0, x_0)||\tau - x_0|^{1+\nu_1+\nu_4+\delta_{i,1}+\delta_{i,4}} \leqslant C_{\phi,\nu'}, \tag{A.8}$$

for all $\tau \in (0, \tau_0)$, with $\tau_0(H_0, \phi_0, x_0) > 0$ small enough. In fact, due to lemma A.2, and the induction hypothesis, we obtain that

$$D^{\nu'}\left(\underline{x}^{N+1}.R\left(\underline{H},\underline{\phi},\underline{x}\right)\right) \to 0, \quad D^{\nu'}\left(\underline{x}^{N-1}.P\left(\underline{H},\underline{\phi},\underline{x}\right)\right) \to 0$$

as $\tau, x_0 \to 0$ for any $C_{H,\nu'}, C_{\phi,\nu'} > 0$. Consequently, by lemma A.3, we find for $\xi > 0$ small enough, that there is a constant $K = K(M, |\Lambda|_{C^M}, |\Omega|_{C^M}, \widetilde{C}_{\nu'})$ depending only on: (a) M, (b) uniform C^M bounds $|\Lambda|_{C^M}$ and $|\Omega|_{C^M}$ of Λ and Ω, respectively, and on (c) $\widetilde{C}_{\nu'}$, such that

$$\left|\frac{d\underline{H}_{\nu'}}{d\tau}\right| \leqslant K,$$
$$\left|\frac{d\underline{\phi}_{\nu'}}{d\tau}\right| \leqslant \underline{x}^{-2-\nu_1-\nu_4-\delta_{i,1}-\delta_{i,4}}K,$$

for all $(\tau, H_0, \phi_0, x_0) \in V(\xi)$ and $\tau \in (0, \tau_0)$. The main observation here is that by taking $\xi > 0$ small enough, we ensure that K is independent of $C_{H,\nu'}$ and $C_{\phi,\nu'}$. We then integrate and use

$$\left|\int_0^\tau \underline{x}^{-q}dt\right| \leqslant \frac{2}{q-1}|\tau - x_0|^{1-q},$$

for any $q > 1$. This produces the following

$$\begin{aligned}
|\underline{H}_{\nu'}(\tau, H_0, \phi_0, x_0)| &\leqslant \widetilde{C}_{\nu'} + |x_0|K,\\
|\underline{\phi}_{\nu'}(\tau, H_0, \phi_0, x_0)| &\leqslant \widetilde{C}_{\nu'}|x_0|^{-1-\nu_1-\nu_4-\delta_{i,1}-\delta_{i,4}}\\
&\quad + \frac{2}{1+\nu_1+\nu_4+\delta_{i,1}+\delta_{i,4}}|\tau - x_0|^{-1-\nu_1-\nu_4-\delta_{i,1}-\delta_{i,4}}K\\
&\leqslant |\tau - x_0|^{-1-\nu_1-\nu_4-\delta_{i,1}-\delta_{i,4}}\left(\widetilde{C}_{\nu'} + \frac{2K}{1+\nu_1+\nu_4+\delta_{i,1}+\delta_{i,4}}\right),
\end{aligned}$$

where we have also used lemma A.5. We now take

$$C_{\phi,\nu'} := \widetilde{C}_{\nu'} + \frac{2K}{1+\nu_1+\nu_4+\delta_{i,1}+\delta_{i,4}},$$

and upon decreasing $\xi > 0$ further, we ensure that $|x_0| \leqslant \frac{\widetilde{C}_{\nu'}}{K}$. Then it follows that (A.8) holds true for all $\tau \in (0, x_0)$ as desired. This completes the proof of lemma A.4.

ORCID iD

K Uldall Kristiansen https://orcid.org/0000-0001-6090-7649

References

[1] Arnold V I 1989 *Mathematical Methods of Classical Mechanics* (Springer)
[2] Balser W 1994 *From Divergent Power Series to Analytic Functions: Theory and Application of Multisummable Power Series* (Springer)
[3] Bittmann A 2018 Doubly-resonant saddle-nodes in (C3,0) and the fixed singularity at infinity in painlevé equations: Analytic classification *Ann. Fourier* **68** 1715–830
[4] Bonckaert P and De Maesschalck P 2008 Gevrey normal forms of vector fields with one zero eigenvalue *J. Math. Anal. Appl.* **344** 301–21
[5] Celletti A 2006 Basics of regularization theory *NATO Science Series II: Mathematics, Physics and Chemistry* vol 227 (Springer) pp 203–30
[6] Celletti A, Stefanelli L, Lega E and Froeschlé C 2011 Some results on the global dynamics of the regularized restricted three-body problem with dissipation *Celest. Mech. Dyn. Astron.* **109** 265–84
[7] Constantine G M and Savits T H 1996 A multivariate Faa di Bruno formula with applications *Trans. Am. Math. Soc.* **348** 503–20

[8] Corne J L and Rouche N 1973 Attractivity of closed sets proved by using a family of liapunov functions *J. Differ. Equ.* **13** 231–46
[9] Diacu F 1999 Two-body problems with drag or thrust: Qualitative results *Celest. Mech. Dyn. Astron.* **75** 1–15
[10] Duignan N and Dullin H R 2020 On the C8/3-regularisation of simultaneous binary collisions in the collinear 4-body problem *J. Differ. Equ.* **269** 7975–8006
[11] Duignan N and Dullin H R 2021 On the C8/3-regularisation of simultaneous binary collisions in the planar four-body problem *Nonlinearity* **34** 4944–82
[12] Dumortier F *et al* 1991 Local study of planar vector fields: Singularities and their unfoldings *Structures in Dynamics, Finite Dimensional Deterministic Studies* vol 2, ed H W Broer (Springer) pp 161–241
[13] Dumortier F 1993 Techniques in the theory of local bifurcations: Blow-up, normal forms, nilpotent bifurcations, singular perturbations *Bifurcations and Periodic Orbits of Vector Fields* (*NATO ASI Series* vol 408) ed D Schlomiuk (Springer) pp 19–73
[14] Dumortier F, Llibre J and Artes J C 2006 *Qualitative Theory of Planar Differential Systems* (Springer)
[15] Dumortier F and Roussarie R 1996 *Canard Cycles and Center Manifolds* vol 121 (Mem. Amer. Math. Soc.) pp 1–96
[16] Elbialy M S 1990 Collision singularities in celestial mechanics *SIAM J. Math. Anal.* **21** 1563–93
[17] Guckenheimer J and Holmes P 1997 *Nonlinear Oscillations, Dynamical Systems and Bifurcations of Vector Fields* 5th edn (Springer)
[18] Hadjidemetriou J D and Voyatzis G 2010 On the dynamics of extrasolar planetary systems under dissipation: migration of planets *Celest. Mech. Dyn. Astron.* **107** 3–19
[19] Haraux A 2021 On some damped 2 body problems *Evol. Equ. Control. Theory* **10** 657–71
[20] Jacobi C G J 2009 *Jacobi's Lectures on Dynamics* (Hindustan Book Agency)
[21] Jelbart S, Kristiansen K U, Szmolyan P and Wechselberger M 2021 Singularly perturbed oscillators with exponential nonlinearities *J. Dyn. Differ. Equ.* **34** 1–53
[22] Jelbart S, Kristiansen K U and Wechselberger M 2021 Singularly perturbed boundary-focus bifurcations *J. Differ. Equ.* **296** 412–92
[23] Kosiuk I and Szmolyan P 2011 Scaling in singular perturbation problems: Blowing up a relaxation oscillator *SIAM J. Appl. Dyn. Syst.* **10** 1307–43
[24] Kosiuk I and Szmolyan P 2015 Geometric analysis of the Goldbeter minimal model for the embryonic cell cycle *J. Math. Biol.* **72** 1337–68
[25] Kristiansen K U 2017 Blowup for flat slow manifolds *Nonlinearity* **30** 2138–84
[26] Kristiansen K U 2020 A new type of relaxation oscillation in a model with rate-and-state friction *Nonlinearity* **33** 2960–3037
[27] Kristiansen K U and Hogan S J 2018 Resolution of the piecewise smooth visible-invisible two-fold singularity in $\mathbb{R}^3$ using regularization and blowup *J. Nonlinear Sci.* **29** 723–87
[28] Kristiansen K U and Ortega R 2023 Circularization in the damped Kepler problem (arXiv:2312.07249)
[29] Kristiansen K U and Szmolyan P 2021 Relaxation oscillations in substrate-depletion oscillators close to the nonsmooth limit *Nonlinearity* **34** 1030–83
[30] Kristiansen K U and Szmolyan P 2022 A dynamical systems approach to WKB-methods: the simple turning point (arXiv:2207.00252v2)
[31] Krupa M and Szmolyan P 2001 Relaxation oscillation and canard explosion *J. Differ. Equ.* **174** 312–68
[32] Llibre J, da Silva P R and Teixeira M A 1997 Regularization of discontinuous vector fields on $\mathbb{R}^3$ via singular perturbation *J. Dyn. Differ. Eq.* **19** 309–31
[33] Margheri A and Misquero M 2020 A dissipative Kepler problem with a family of singular drags *Celest. Mech. Dyn. Astron.* **132** 17
[34] Margheri A, Ortega R and Rebelo C 2012 Some analytical results about periodic orbits in the restricted three body problem with dissipation *Celest. Mech. Dyn. Astron.* **113** 279–90
[35] Margheri A, Ortega R and Rebelo C 2014 Dynamics of Kepler problem with linear drag *Celest. Mech. Dyn. Astron.* **120** 19–38

[36] Margheri A, Ortega R and Rebelo C 2017 First integrals for the Kepler problem with linear drag *Celest. Mech. Dyn. Astron.* **127** 35–48
[37] Margheri A, Ortega R and Rebelo C 2017 On a family of Kepler problems with linear dissipation *Rend. Istit. Mat. Univ. Trieste* **49** 265–86
[38] Martinez R and Simó C 1999 Simultaneous binary collisions in the planar four-body problem *Nonlinearity* **12** 903–30
[39] McGehee R 1974 Triple collision in the collinear three-body problem *Invent. Math.* **27** 191–227
[40] Poincaré H 1911 *Leçons Sur les Hypothéses Cosmogoniques* (Libraire scientifique A. Hermann et fils)